**Doctoral Dissertation**

# Mouse embryonic dorsal root ganglia contain pluripotent stem cells that show features similar to embryonic stem cells (ES cells) and induced pluripotent stem cells (iPS cells)

## マウス胚後根神経節は胚性幹細胞(ES 細胞)および人工多能性幹細胞(iPS 細胞)と同様の特徴を示す多能性幹細胞を含む

**Ryuhei Ogawa**

**Department of Biological Sciences**
**Graduate School of Science**
**Osaka University**

**August 2017**

**CONTENTS**

## List of Figures

## List of Tables

**Page**

## Abbreviations

| | |
|---|---|
| ℃ | degrees Celsius |
| α-MEM | α-modified minimum essential medium |
| μChIP | micro chromatin immunoprecipitation |
| μg | microgram |
| μm | micrometer |
| μM | micromolar |
| μl | microliter |
| Blimp1 | B lymphocyte-induced maturation protein 1 |
| BMP | bone morphogenetic protein |
| CEE | extract of day-11 chick embryos |
| CHD7 | chromodomain helicase DNA-binding protein 7 |
| CO2 | carbon dioxide |
| DAPI | 4',6-diamidino-2-phenylindole |
| DN | dominant-negative |
| DNA | deoxyribonucleic acid |
| DRG | dorsal root ganglion |
| E | embryonic day |
| EB | embryoid body |
| EDTA | ethylenediaminetetraacetic acid |

| | |
|---|---|
| EGF | epidermal growth factor |
| EGTA | ethylene glycol bis (2-aminoethyl ether)-N,N,N’,N’-tetraacetic acid |
| ES cells | embryonic stem cells |
| FA | formaldehyde |
| FBS | fetal bovine serum |
| FGF2 | fibroblast growth factor 2 |
| Foxa2 | forkhead box protein A2 |
| GFAP | glial fibrillary acidic protein |
| h | hours |
| HCl | hydrogen chloride |
| IgG | immunoglobulin G |
| IgM | immunoglobulin M |
| iPS cells | induced pluripotent stem cells |
| min | minutes |
| ml | milliliter |
| mm | millimeter |
| mM | millimolar |
| NaBu | sodium butyrate |
| NaCl | sodium chloride |
| NCSCs | neural crest-derived stem cells |
| NF | neurofilament L |
| ng | nanogram |

| | |
|---|---|
| nM | nanomolar |
| NT | neural tube |
| Oct4 | octamer-binding transcription factor 4 |
| PBS | phosphate buffered saline |
| PCNA | proliferating cell nuclear antigen |
| PFA | paraformaldehyde |
| PGCLCs | primordial germ cell-like cells |
| PSCs | pluripotent stem cells |
| qPCR | quantitative real-time polymerase chain reaction |
| RIPA | radio-immunoprecipitation assay |
| s | seconds |
| SDS | sodium dodecyl sulfate |
| s.e.m. | standard error of the mean |
| siRNA | small interfering ribonucleic acid |
| SMA | α smooth muscle cell actin |
| Sox | SRY-related HMG-box gene |
| SSEA1 | stage-specific embryonic antigen 1 |
| TE | Tris-EDTA |
| TGFβ | transforming growth factor-β |
| Tris | Tris (hydroxymethyl) aminomethane |
| LIF | leukemia inhibitory factor |
| WT | wild-type |

## SUMMARY

The neural crest is a transient embryonic structure that originates from the neural fold during vertebrate development. Neural crest cells differentiate into ectodermal and mesodermal cell types. Some of the neural crest cells maintain their multipotency and form neural crest-derived stem cells (NCSCs). Buitrago-Delgado et al. [Science 348, 1332-1335 (2015)] have suggested that *Xenopus* neural crest cells are pluripotent cells which generate not only ectodermal and mesodermal features, but also endodermal features. Therefore, we examined whether or not NCSCs have developmental potentials equivalent to those of pluripotent stem cells (PSCs).

In the present study, since there are no ways to isolate only NCSCs, we used the neural crest-derived dorsal root ganglion (DRG) that was dissected from the mouse embryo for investigating of the properties of NCSCs. Therefore, we cannot exclude the possibility that the isolated DRGs may contain non-DRG cells derived from surrounding tissues. Bearing this caveat in my mind, we drew the following conclusions. Mouse embryonic DRGs contains PSCs that may have developmental capacities equivalent to those of embryonic stem (ES) cells and induced pluripotent stem cells. Mouse embryonic DRG cells expressed pluripotency-related transcription factors [octamer-binding transcription factor 4, SRY (sex determining region Y)-box containing gene (Sox) 2, and Nanog] that play essential roles in maintaining the pluripotency of ES cells. Furthermore, the DRG cells differentiated into ectoderm-,

mesoderm- and endoderm-derived cell types. These cells produced primordial germ cell-like cells and embryoid body-like spheres. The combination of leukemia inhibitor factor/bone morphogenetic protein 2/fibroblast growth factor 2 effectively promoted maintenance of the pluripotency of the PSCs present in DRGs, as well as that of neural crest-derived stem cells (NCSCs) in DRGs. NCSCs expressed chromodomain helicase DNA-binding protein 7 (CHD7) and Sox10, and differentiated into smooth muscle cells, neurons, and glia. The expression of pluripotency-related transcription factors in the DRG cells was regulated by CHD7 and Sox10, which are indispensable for the formation of NCSCs, and vice versa. These findings support the possibility that PSCs in mouse embryonic DRGs are NCSCs and suggest that pluripotency at the early stage of mouse embryonic development is inherited by mouse NCSCs.

# INTRODUCTION

The neural crest is a transient embryonic structure that originates from the neural fold, the boundary area between neural ectoderm and non-neural ectoderm, during vertebrate development (Fig. 1A). Neural crest cells migrate to various embryonic regions, where they differentiate into a wide range of cells, including peripheral neurons and glia, melanocytes, chondrocytes, smooth muscle cells, endocrine cells, and adipocytes (Fig. 1B; Hall, 1999; Le Douarin and Kalcheim, 1999; Bronner, et al 2015). Furthermore, a recent investigation reported that *Xenopus* neural crest cells generate not only ectodermal and mesodermal features, but also endodermal features (Fig. 1C; Buitrago-Delgado et al., 2015). Thus, neural crest cells may be pluripotent cells (De Los Angeles et al., 2015).

Although some of the neural crest cells undergo developmental restrictions, some instead maintain their multipotency even after having entered target tissues (Motohashi et al., 2014) and form NCSCs, typical tissue-specific stem cells (Fig. 2A; Shakhova and Sommer, 2010; Achilleos and Trainor, 2012; Dupin and Sommer, 2012; Sieber-Blum, 2012). It has been reported that NCSCs exist in late embryonic and adult tissues such as DRG (Hagedorn et al., 1999; Paratore et al., 2002; Li et al., 2007), sciatic nerve (Morrison et al., 1999; Joseph et al., 2004), gut (Kruger et al., 2002; Bixby et al., 2002), bone marrow (Nagoshi et al., 2008), cornea (Yoshida et al., 2006), heart (Tomita et al., 2005), and skin (Sieber-Blum et al., 2004; Wong et al., 2006). Our previous study

suggested that CHD7, Sox10, and Wnt3a/BMP2 signaling play essential roles in the formation of NCSCs (Fig. 2B; Fujita et al., 2014). Mammalian neural crest cells (Thomas et al., 2008; Fujita et al., 2014; Hagiwara et al., 2014) and mammalian early embryonic pluripotent cells (Nichols et al., 1998; Avilion et al., 2003; Mitsui et al., 2003) express CHD7 and/or pluripotency-related transcription factors (Fig. 2B,D), including Oct4, Sox2, and Nanog, and these factors play important roles in the maintenance of pluripotency of ES cells (Niwa, 2007). Pluripotency-related transcription factors colocalize at CHD7 binding sites of target gene enhancers in mouse ES cells (Fig. 2C; Schnetz et al., 2010). These reports suggest that pluripotency at the early stage of embryonic development is inherited by neural crest cells and NCSCs. Thus, NCSCs may be PSCs (Fig. 2D). This means that there may exist PSCs until much later developmental stages than those thought conventionally. Additionally, several types of tissue-specific stem cells show multipotency. They have been shown to be present in bone marrow (D'Ippolito et al., 2004), oral mucosa (Marynka-Kalmani et al., 2010), dental pulp (Atari et al., 2011), adipose tissue (Jumabay et al., 2014), and skeletal muscle (Vojnits et al., 2015).

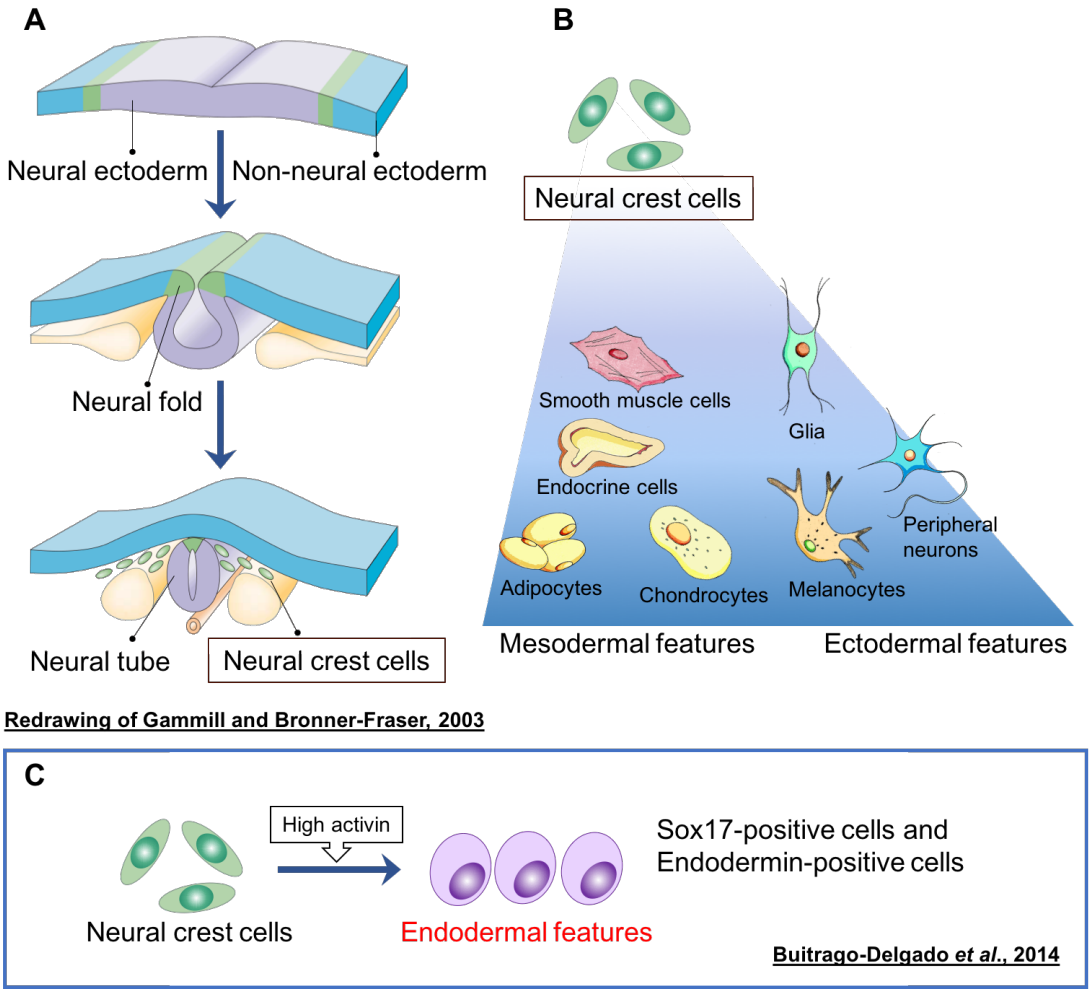


**Fig. 1**

**Development of the neural crest.**

(A) The neural crest originates from the neural fold (green), the boundary of the neural ectoderm (blue) and the non-neural ectoderm (purple). Neural crest cells delaminate from the neural fold and migrate throughout the embryo. (B) Neural crest cells differentiate into various cell types, such as melanocytes, peripheral neurons and glia, chondrocytes, endocrine cells, and adipocytes. (C) *Xenopus* neural crest cells differentiate into endodermal cells that express Sox17 and Endodermin in the presence of high concentration activin A.

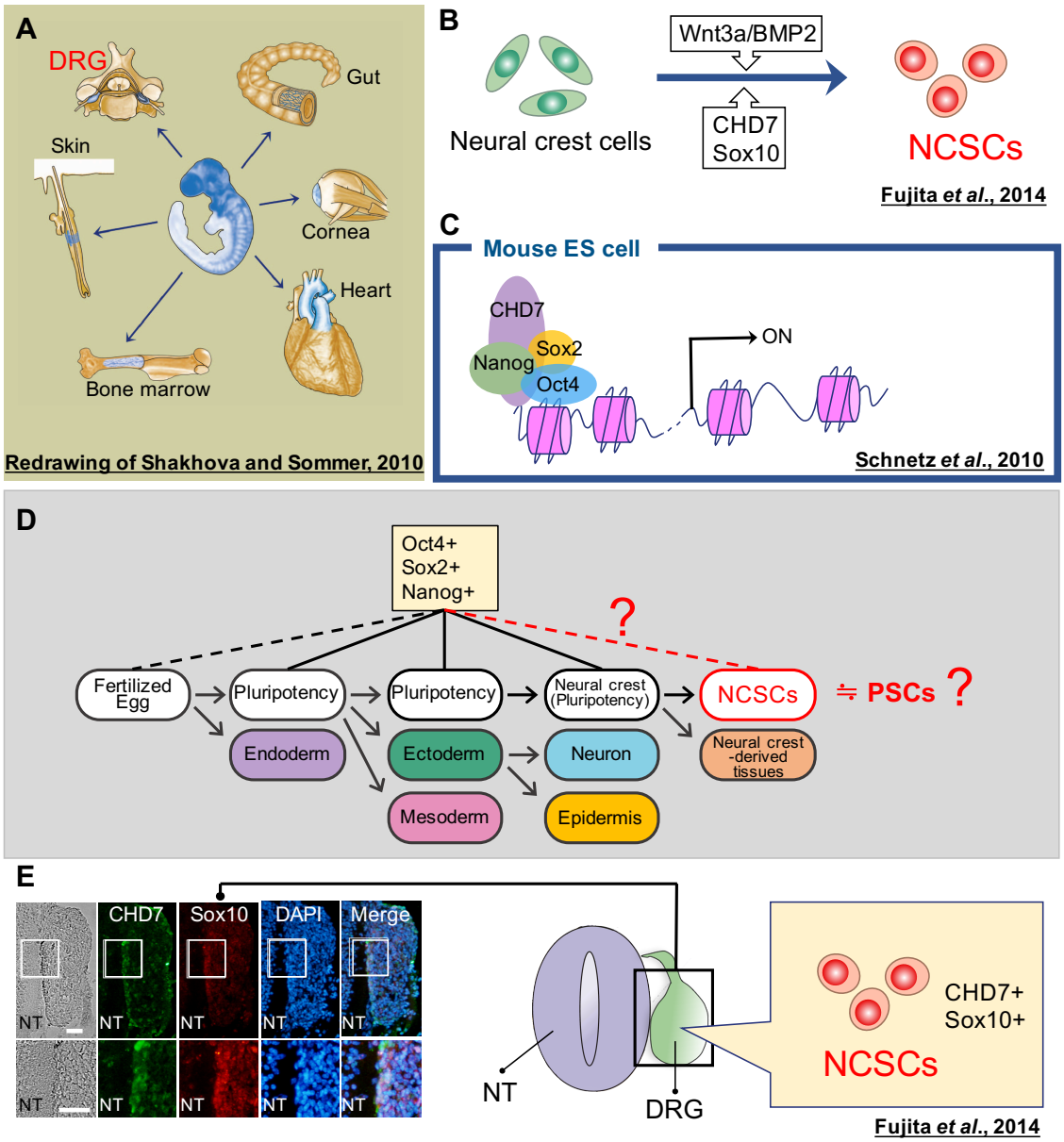


**Fig. 2**

**Relationship between NCSCs and PSCs.**

(A) NCSCs are present in various adult tissues including DRG, gut, cornea, heart, bone marrow, and skin. (B) Wnt3a/BMP2, CHD7, and Sox10 play essential roles in the formation of mouse NCSCs. (C) CHD7, Oct4, Sox2, and Nanog colocalize at binding sites of target gene enhancers in mouse ES cells.

(D) Mammalian early embryonic pluripotent cells and mammalian neural crest cells express pluripotency-related transcription factors. Thus, the pluripotency of the early embryonic pluripotent cells may be handed over to neural crest cells and then NCSCs. (E) Expression pattern of CHD7 and Sox10, the factors which characterize NCSCs, in transverse sections of E12 mouse DRGs. The top, bottom, left, and right of each photograph correspond to the dorsal, ventral, proximal, and distal side of the embryo, respectively. Scale bars: 20 μm.

---

We showed that E12 mouse DRGs contain NCSCs which coexpressed CHD7 and Sox10 (Fig. 2E; Fujita et al., 2014). Seventy percent of adult mouse DRG-derived cell spheres contain NCSCs, while only 3 to 7% of cell spheres that originate from other neural crest-derived tissues contain NCSCs (Nagoshi et al., 2008). In the present study, therefore, we investigated mouse embryonic DRGs to determine whether or not the DRGs contain PSCs, what conditions are essential for the maintenance of NCSCs and PSCs in the DRGs, and what correlation exists between PSCs and NCSCs in the DRGs.

# MATERIALS AND METHODS

## Animals

We used pregnant ddY mice and 4–5-week-old KSN/Slc athymic nude mice (male) in the present study. ddY and nude mice were purchased from Japan SLC, Inc (Shizuoka, Japan). The mouse experiments were approved by the Animal Experimentation Committee of Osaka University. Mice were treated humanely, and all mouse experiments were made under conditions designed to minimize suffering.

## Isolation of mouse embryonic DRGs

E12 mouse embryonic DRGs were dissected according to methods described previously (Hall, 2006). Liver, gut, and tail were removed by using sharp forceps, leaving a vertebral column. The cartilaginous ventral structure of a vertebral column was broken open, and then the neural tube with attached DRGs and dorsal skin was dissected. This tissue between the forelimb and the hindlimb was cut by using scissors. Dorsal skin was peeled off with fine forceps, and the neural tube with attached DRGs was taken out. DRGs were isolated from the neural tube with attached DRGs using tungsten needle.

**Explant cultures**

Explant cultures of mouse embryonic DRGs were performed as described previously (Fujita et al., 2014). The isolated DRGs were explanted into 35-mm culture dishes coated with collagen gel (Cellmatrix, Nitta Gelatin, Osaka, Japan). The cultures were incubated at 37°C in a humidified atmosphere containing 5% CO2, and the culture medium (see the '**Culture medium and signaling molecules**' section) was changed every other day.

**Suspension cultures**

DRGs were dissociated according to a modification of methods described previously (Murphy et al., 1991; Hjerling-Leffler et al., 2007). The isolated DRGs were minced and then incubated in 0.025% trypsin and 0.02% EDTA for 12 min at 37°C. For suspension cultures, the dissociated DRG cells were triturated using fire-polished Pasteur pipettes until they formed a single-cell suspension (>95% single cells). The cell suspension was seeded at 2000 cells/well onto a wall of a low-adhesion surface U-bottom 96-well plate (IWAKI, Tokyo, Japan) to examine the formation of EB-likes spheres. The cultures were incubated at 37°C in a humidified atmosphere containing 5% CO2, and the culture medium (see the '**Culture medium and signaling molecules**' section) was added 75 μl per 2 days.

**Clonal cultures**

Clonal cultures of mouse embryonic DRG cells were performed by a modification of methods described previously (Ito et al., 1993). DRGs were dissected and cut into small fragments. These fragments were explanted into 35-mm culture dishes coated with collagen gel (Cellmatrix, Nitta Gelatin). Two days later, DRG cells derived from these fragments were resuspended by trypsinization. This essentially single cell suspension (>95% single cells) was diluted to 100 cells/ml. One milliliter aliquots of this diluted cell suspension were plated to 35-mm culture dishes that were coated with a collagen gel (PureCol, Advanced BioMatrix, SanDiego, USA) and conditioned with culture medium (see the '**Culture medium and signaling molecules**' section) containing 10 μg/ml plasma fibronectin (Sigma, St. Louis, USA). The clone founder cells were identified at 8 h after seeding cells. The cultures were incubated at 37°C in a humidified atmosphere containing 5% CO2, and the culture medium was changed every day for the first 2 days and then every other day.

**Culture medium and signaling molecules**

The culture medium consisted of 85% α-MEM (Sigma), 10% FBS (GE Healthcare Life Sciences, Pittsburgh, USA), 5% CEE, and 50 μg/ml gentamicin (Sigma). We used 1% or 10% Nu-serum (Becton Dickinson, Lincoln Park, USA) instead of FBS and CEE in the formation of PGCLCs.

LIF (Wako, Osaka, Japan) was added to the medium at 1000 units/ml. Wnt3a (PeproTech, Rocky Hill, USA), BMP2 (R&D Systems, Minneapolis, USA), BMP4 (a gift from the Genetic Institute, Andover, USA), FGF2 (R&D Systems, PeproTech), EGF (PeproTech), TGFβ (PeproTech), and activin A (PeproTech) were used at 10 ng/ml, 10 ng/ml, 10 ng/ml, 10 ng/ml, 2-10 ng/ml, 0.1 ng/ml, and 100 ng/ml, respectively.

**Transfection of expression vectors and siRNAs**

Mouse embryonic DRG cells in explant cultures were transfected with 1 μg of the following expression vectors: (1) pcDNA3.1 encoding human WT CHD7 and a Flag-6×His tag (a gift from Dr J. Wysocka, Stanford University, Stanford, USA; Bajpai et al., 2010), (2) pcDNA3.1 encoding human DN CHD7 and a Flag-6×His tag (a gift from Dr J. Wysocka; Bajpai et al., 2010). Transfection was performed using Lipofectamine 2000 (Invitrogen, Carlsbad, USA) for the first 48 h in culture.

The siRNA duplexes for *CHD7*, *Oct4*, *Sox2*, and *Nanog* were designed based on their sequences published online (GenBank Accession Nos. NM_001081417, NM_013633, NM_011443, NM_028016). All siRNA sequences are listed in Table 1. Stealth™RNAi Negative Control Medium GC Duplex #2 (Invitrogen) was used as the control for *CHD7*, *Oct4*, *Sox2*, or *Nanog* siRNA. Using Lipofectamine 2000, mouse embryonic DRG cells were transfected with 40 nM *CHD7* siRNA, *Oct4* siRNA, *Sox2* siRNA, *Nanog* siRNA, or the RNAi Negative Control for the first 48 h in culture.

**Table 1: siRNA sequences**

| Gene | Sequence (5' to 3') |
|---|---|
| *CHD7* | CAGGCUCAAGCUAGAUGCCACAGAA |
| *Oct4* | CCGGAAGAGAAAGCGAACUAGCAUU |
| *Sox2* | UUUAUAAUCCGGGUGCUCCUUCAUG |
| *Nanog* | UUAUAGCUCAGGUUCAGAAUGGAGG |

**Immunostaining**

Explant and clonal cultures were fixed with 4% PFA for 1 h on ice. The cultures were immunostained with the primary antibodies for 16 h at 4°C, except in the case of immunostaining with anti-Nanog (Santa Cruz, Dallas, USA, sc-30328), which was performed for 1 h at 37°C. The cultures were treated with secondary antibodies for 1 h at room temperature.

Neural tubes with attached DRGs were fixed with 4% PFA for 1 h on ice. The fixed tissues were immersed in gradually increasing concentrations of sucrose solution and embedded in OCT compound (Miles, Elkhart, USA). Cryostat sections were cut at 10 μm and mounted on albumin-coated glass slides. The sections were immunostained with primary antibodies for 16 h at 4°C and then treated with secondary antibodies for 1 h at room temperature. Finally, the nuclei in cultures and sections were stained with 0.1 μg/ml DAPI (Dojindo, Kumamoto, Japan). DAPI nuclear staining was important for counting the exact number of immunoreactive cells in the DRG cell cultures and for judging cell death. Details of all antibodies used are listed in Table 2.

**Table 2: Antibodies used for immunostaining**

| **Antibodies used for Immunostaining** | | |
|---|---|---|
| **Antigen/Conjugation** | **Dilution** | **Catalog number** |
| Oct4 (rabbit polyclonal antibody) | 1:1000 | Santa Cruz (sc-9081 X) |
| Sox2 (goat polyclonal antibody) | 1:1000 | Santa Cruz (sc-17320 X) |
| Nanog (goat polyclonal antibody) | 1:200 | Santa Cruz (sc-30328) |
| Nanog (5A10, mouse monoclonal IgG2a) | 1:100 | Santa Cruz (sc-134218) |
| SSEA1 (MC480, mouse monoclonal IgM) | 1:100 | Cell Signaling (4744) |
| Neurofilament 68 (NF68; rabbit polyclonal antibody) | 1:500 | MILLIPORE (AB9568) |
| GFAP (rabbit polyclonal antibody) | 1:100 | DAKO (Z0334) |
| α-smooth muscle actin (SMA; 1A4, mouse monoclonal IgG2a) | 1:800 | Sigma (A2547) |
| Collagen type II (goat polyclonal antibody) | 1:50 | Southern Biotechnology (1320-01) |
| Sox17 (goat polyclonal antibody) | 1:100 | Santa Cruz (sc-17355) |
| Foxa2 (goat polyclonal antibody) | 1:100 | Santa Cruz (sc-6554) |
| CHD7 (goat polyclonal antibody) | 1:50 or 1:100 | Santa Cruz (sc-79207) |
| Sox10 (rabbit polyclonal antibody) | 1:100 | MILLIPORE (AB5727) |
| Blimp1 (3H2E8, mouse monoclonal IgG1) | 1:50 | Santa Cruz (sc-66015) |
| PCNA (PC10, mouse monoclonal IgG2a) | 1:100 | Santa Cruz (sc-56) |
| Caspase-3 (C-6, mouse monoclonal IgG1) | 1:100 | Santa Cruz (sc-271759) |
| Alexa Fluor 488 (Donkey anti-Rabbit IgG) | 1:500 | Invitrogen (A-21206) |
| Alexa Fluor 555 (Donkey anti-Rabbit IgG) | 1:500 | Invitrogen (A-31572) |
| Alexa Fluor 488 (Donkey anti-Goat IgG) | 1:500 or 1:1000 | Invitrogen (A-11055) |
| Alexa Fluor 555 (Donkey anti-Goat IgG) | 1:500 | Invitrogen (A-21432) |
| Alexa Fluor 488 (Donkey anti-Mouse IgG) | 1:500 | Invitrogen (A-21202) |
| Fluorescein (FITC)-conjugated AffiniPure Donkey anti-Mouse IgM | 1:100 | Jackson ImmunoResearch (715-095-140) |

**Alkaline phosphatase staining**

Neural tubes with attached DRGs were fixed with 4% PFA for 1 h on ice, and then were cut at 10 μm as cryostat sections. These sections were stained by using alkaline phosphatase staining kit (Wako, 294-67001).

**Teratoma formation assay**

Approximately $5x10^5$ or $10x10^5$ dissociated DRG cells in 50% Cultex BME (Trevigen, Gaithersburg, USA, 3432-001-01) were injected subcutaneously into the dorsal flank of athymic nude mice. The dissociated DRG cells were prepared under the following three different conditions: (1) cells dissociated from mouse E12 DRGs, (2) cells dissociated from the DRG explants cultured for 6 days under the control condition that did not contain any signaling molecules, or (3) cells dissociated from the DRG explants cultured for 6 days under conditions containing LIF/BMP2/FGF2. The animals were sacrificed 2 or 3 months after the injection and tumors were dissected.

**Histology**

Teratomas were fixed with Bouin's fixative and embedded in paraffin. The paraffin sections were cut at 7 μm and mounted on albumin-coated glass slides. After deparaffinization, the sections were stained with Ehrlich's hematoxylin and

counterstained with eosin and Alcian Blue (pH 2.6). Several teratomas were fixed with 4% PFA for 1 h on ice for immunostaining. These teratomas were treated as described above (see the '**Immunostaining**' section) and then immunostained.

**µChIP-qPCR analysis**

µChIP was performed by a modification of methods described previously (Dahl and Collas, 2008). Mouse embryonic DRGs or DRG cells in explant cultures were dissociated by trypsinization and subsequently triturated using fire-polished Pasteur pipettes until a single-cell suspension (>95% single cells) was obtained.

The chromatin in these cells was cross-linked by adding formaldehyde at a final concentration of 1% for 8 min at room temperature. The crosslinked cells were washed with phosphate buffered saline containing 20 mM NaBu. The pellets of these cells were resuspended and lysed in lysis buffer [1% SDS, 10 mM EDTA, 50 mM Tris-HCl, pH 8.0, 20 mM NaBu, and protease inhibitor tablet (Complete Protease Inhibitor Mini EDTA-free, Roche, Basel, Switzerland)] for 5 min on ice. The lysate was diluted fivefold with RIPA buffer [0.1% SDS, 1 mM EDTA, 10 mM Tris-HCl, pH 8.0, 150 mM NaCl, 0.5 mM EGTA, 0.1% Na-deoxycholate, 1% Triton X-100, and protease inhibitor tablet] and sonicated using an Advanced Sonifier 250A at output 2, duty cycle 60% for 4Å~10 s pulses each with a 2 min pause between pulses on ice.

Chromatin fragments were incubated for 2 h at 4°C with 10 µl of Protein G-coated paramagnetic beads that had been preincubated with the appropriate antibodies.

The antibodies used for immunoprecipitation are listed in Table 3. The complexes were washed twice with RIPA buffer and once with TE, and were eluted in elution buffer [1% SDS, 20 mM Tris-HCl, pH 8.0, 50 mM NaCl, 5 mM EDTA, and 20 mM NaBu] from the beads by heating at 65°C with occasional vortexing. The cross-linking was reversed by incubation at 65°C overnight. DNA was purified by treatment with Proteinase K (0.2 mg/ml; Wako) and phenol/chloroform/isoamyl alcohol.

**Table 3: Antibodies used for μChIP**

| Antigen | Amount | Catalog number |
|---|---|---|
| Oct4 (rabbit polyclonal antibody) | 5 μg | Santa Cruz (sc-9081 X) |
| Sox2 (goat polyclonal antibody) | 5 μg | Santa Cruz (sc-17320 X) |
| Nanog (D1G10, rabbit monoclonal IgG) | 5 μl | Cell Signaling (8785) |

All qPCR reactions were carried out using ABI7300. The reactions were performed in duplicate for each sample. The primer sets were designed using Primer Express 3.0 (Invitrogen) for *Oct4* promoter conserved region 4 (CR4; Nordhoff et al., 2001), *Sox2* enhancer Sox regulatory regions 2 (SRR2; Tomioka et al., 2002), and *Nanog* promoter (Tanimura et al., 2013). These regions contain Oct-Sox elements and participate in regulating the pluripotency of mouse ES cells (Chew et al., 2005; Tanimura et al., 2013). The primer sequences used for qPCR are shown in Table 4.

**Table 4: Primers used for qPCR**

| Primer name | Sequence (5' to 3') |
|---|---|
| *Oct4* promoter CR4 fwd | AGACGGCAGATGCATAACAAAG |
| *Oct4* promoter CR4 rev | AGCAGATTAAGGAAGGGCTAGGA |
| *Sox2* enhancer SRR2 fwd | GGCTCGGGCAGCCATT |
| *Sox2* enhancer SRR2 rev | ACTGTCGACTGTGCTCATTACCA |
| *Nanog* promoter fwd | CCCAGTCTGGGTCACCTTACA |
| *Nanog* promoter rev | CAGGGTCCACCATGGACATT |

**Statistical analysis**

The significance of differences was determined using Student's t-test. $P<0.05$ was considered statistically significant.

# RESULTS

## Expression of pluripotency-related transcription factors and SSEA1 and activity of alkaline phosphatase in mouse embryonic DRGs

We examined the expression of pluripotency-related transcription factors and SSEA1 and the activity of alkaline phosphatase in E12 mouse DRGs. SSEA1 and alkaline phosphatase activity have been shown to be pluripotency markers in mouse ES and iPS cells (Wobus et al., 1984; Cui et al., 2004; Takahashi and Yamanaka, 2006). The DRG cells expressed Oct4 (Fig. 3B,E,G,J,L,O), Sox2 (Fig. 3C,E), Nanog (Fig. 3H,J) and/or SSEA1 (Fig. 3M,O). Furthermore, the DRGs contained cells expressing both Oct4 and Sox2 (white arrowheads in Fig. 3B′-E′), both Oct4 and Nanog (white arrowheads in Fig. 3G′-J′), or both Oct4 and SSEA1 (white arrowheads in Fig. 3L′-O′). Some of the DRG cells showed alkaline phosphatase activity (Fig. 3P,P′).

## Developmental capacities of mouse embryonic DRG cells

We examined the developmental potentials of mouse embryonic DRG cells in culture. Since it has been reported that BMP4, FGF2, and TGFβ are factors that promote differentiation into neurons (Ota and Ito, 2006), glia (Ota and Ito, 2006), chondrocytes (Ido and Ito, 2006), and smooth muscle cells (John et al., 2011),

respectively; we tested the effects of these factors when added to the culture medium (Fig. 4A). The DRG cells in explant cultures differentiated into neurons (Fig. 4B-E) in BMP4-treated cultures, into glia (Fig. 4F-I) in FGF2-treated cultures, into smooth muscle cells (Fig. 4J-M) in TGFβ-treated cultures, and into chondrocytes (Fig. 4N-Q) in FGF2-treated cultures. Activin A promotes differentiation into endoderm that expresses Sox17 and Foxa2, markers of endodermal cells in the mouse (Besnard et al., 2004; Park et al., 2006; Zorn and Wells, 2009), in mouse ES cells (Yasunaga et al., 2005; Schroeder et al., 2012). Therefore, we examined whether the DRG cells could differentiate into endoderm in the presence of activin A. Activin A-treated DRG cells indeed differentiated into endodermal cells expressing Sox17 (Fig. 4R-U) or Foxa2 (Fig. 4V-Y).

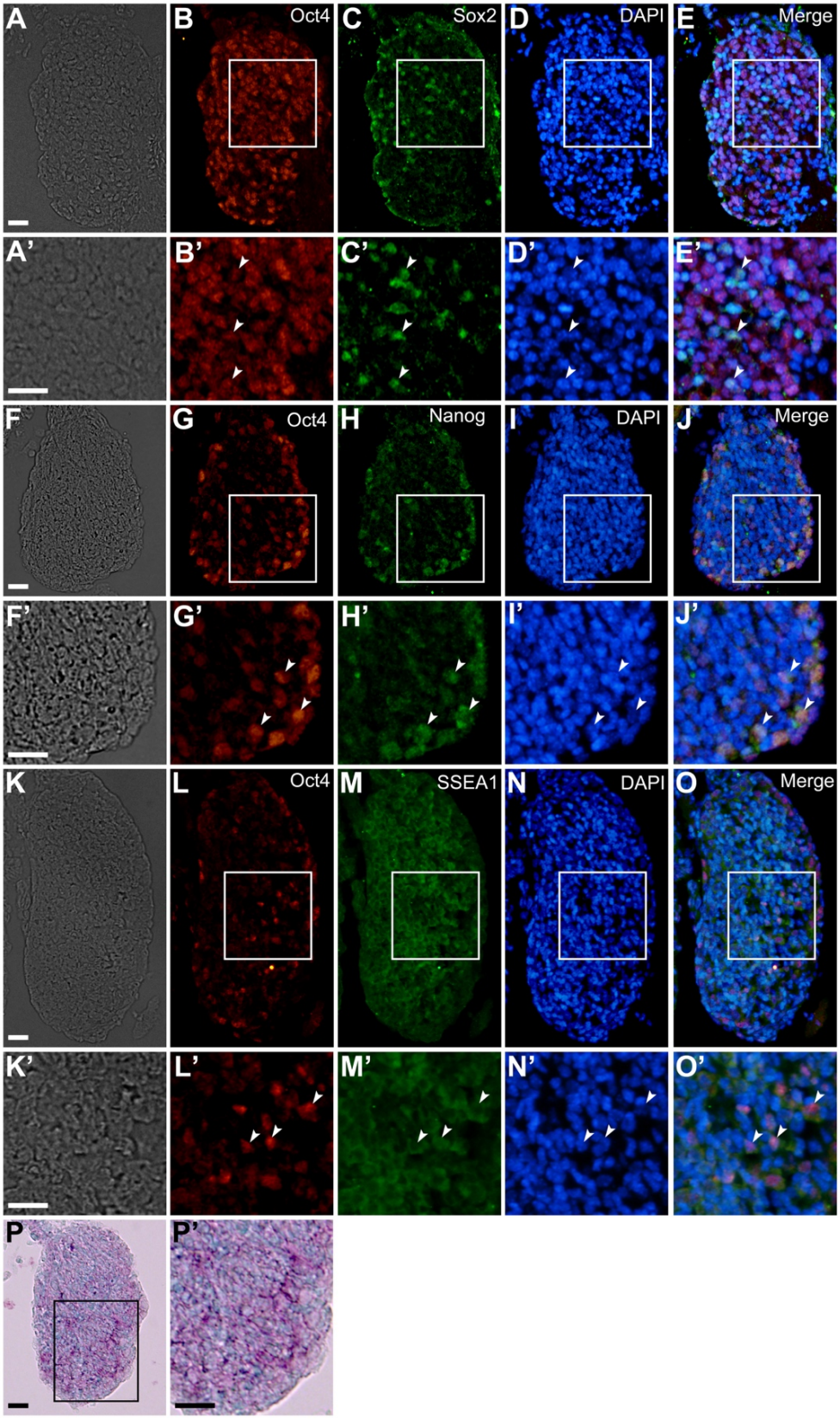
A
B
Oct4
C
Sox2
D
DAPI
E
Merge
A'
B'
C'
D'
E'
F
G
Oct4
H
Nanog
I
DAPI
J
Merge
F'
G'
H'
I'
J'
K
L
Oct4
M
SSEA1
N
DAPI
O
Merge
K'
L'
M'
N'
O'
P
P'

**Fig. 3**

**Expression patterns of Oct4, Sox2, Nanog, and SSEA1 and activity of alkaline phosphatase in mouse embryonic DRGs.**

(A-O) Transverse sections of E12 mouse DRGs. The top, bottom, left, and right of each photograph correspond to the dorsal, ventral, proximal, and distal side of the embryo, respectively. (A) Bright-field image. (B) Expression pattern of Oct4 in the same field as A. (C) Expression pattern of Sox2 in the same field as A. (D) DAPI nuclear staining of the same field as A. (E) Merged image of B-D. (F) Bright-field image. (G) Expression pattern of Oct4 in the same field as F. (H) Expression pattern of Nanog in the same field as F. (I) DAPI nuclear staining of the same field as F. (J) Merged image of G-I. (K) Bright-field image. (L) Expression pattern of Oct4 in the same field as K. (M) Expression pattern of SSEA1 in the same field as K. (N) DAPI nuclear staining of the same field as K. (O) Merged image of L-N. (P) Alkaline phosphatase activity (purple) in mouse embryonic DRGs. Nuclei were stained by methyl green (blue). A′-E′,F′-J′,K′-O′, and P′ show enlarged images of boxed regions in A-E,F-J,K-O, and P, respectively. White arrowheads indicate cells expressing both Oct4 and Sox2 (B′-E′), both Oct4 and Nanog (G′-J′), and both Oct4 and SSEA1 (L′-O′). Scale bars: 20 μm.

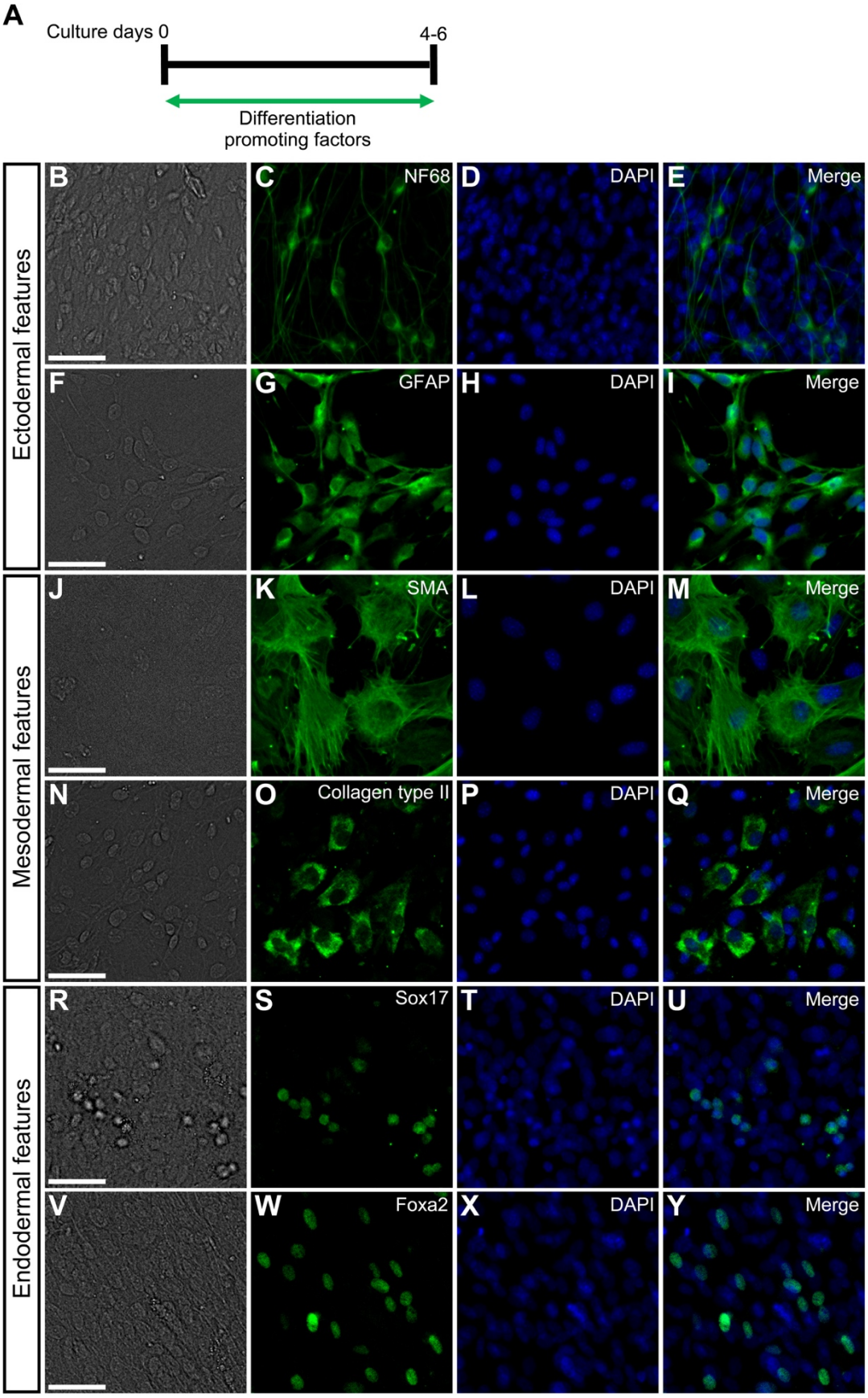
A
Culture days 0
4-6
Differentiation
promoting factors
Ectodermal features
Mesodermal features
Endodermal features
B
C
NF68
D
DAPI
E
Merge
F
G
GFAP
H
DAPI
I
Merge
J
K
SMA
L
DAPI
M
Merge
N
O
Collagen type II
P
DAPI
Q
Merge
R
S
Sox17
T
DAPI
U
Merge
V
W
Foxa2
X
DAPI
Y
Merge

**Fig. 4**

**Developmental capacities of mouse embryonic DRG cells in explant cultures.**

(A) E12 mouse DRG explants were exposed to various differentiation promoting factors for 4 or 6 days. Immunostaining was performed by using anti-NF68, anti-GFAP, anti-SMA, anti-Collagen type II, anti-Sox17, or anti-Foxa2 on culture day 4 or 6. (B) Bright-field image. (C) Anti-NF68-positive cells in the same field as B. (D) DAPI nuclear staining of the same field as B. (E) Merged image of C and D. (F) Bright-field image. (G) Anti-GFAP-positive cells in the same field as F. (H) DAPI nuclear staining of the same field as F. (I) Merged image of G and H. (J) Bright-field image. (K) Anti-SMA positive cells in the same field as J. (L) DAPI nuclear staining of the same field as J. (M) Merged image of K and L. (N) Bright-field image. (O) Anti-Collagen type II-positive cells in the same field as N. (P) DAPI nuclear staining of the same field as N. (Q) Merged image of O and P. (R) Bright-field image. (S) Anti-Sox17-positive cells in the same field as R. (T) DAPI nuclear staining of the same field as R. (U) Merged image of S and T. (V) Bright-field image. (W) Anti-Foxa2-positive cells in the same field as V. (X) DAPI nuclear staining of the same field as V. (Y) Merged image of W and X. Scale bars: 50 μm.

We performed clonal culture analysis to investigate the developmental capacities of single DRG cells. We previously reported that the DRG cells could differentiated into smooth muscle cells even in the absence of TGFβ (Fujita et al., 2014). In clonal cultures, therefore, we did not use TGFβ to induce the differentiation into smooth muscle cells. We detected clones containing both smooth muscle cells (Fig. 5A,D) and neurons (Fig. 5B,D) in BMP4-treated cultures. We also found clones containing both smooth muscle cells (Fig. 5E,H) and endodermal cells expressing Foxa2 (Fig. 5F,H) in activin A-treated cultures. Clones containing cells which express both GFAP and Foxa2 (Fig. 5I,J,L) appeared in the presence of activin A and FGF2. However, no cells expressing Foxa2 only were observed under this condition. This may be due to the addition of both activin A and FGF2.

We investigated the *in vivo* developmental capacities of the DRG cells by using a teratoma formation assay. When 4–5-week-old athymic nude mice were injected with dissociated DRG cells, teratomas were formed (Fig. 6A). The teratomas contained ectoderm-derived cell types (Fig. 6B,C), mesoderm-derived cell types (Fig. 6D-I), and endodermal cells expressing Sox17 (Fig. 6J-M) or Foxa2 (Fig. 6N-Q).

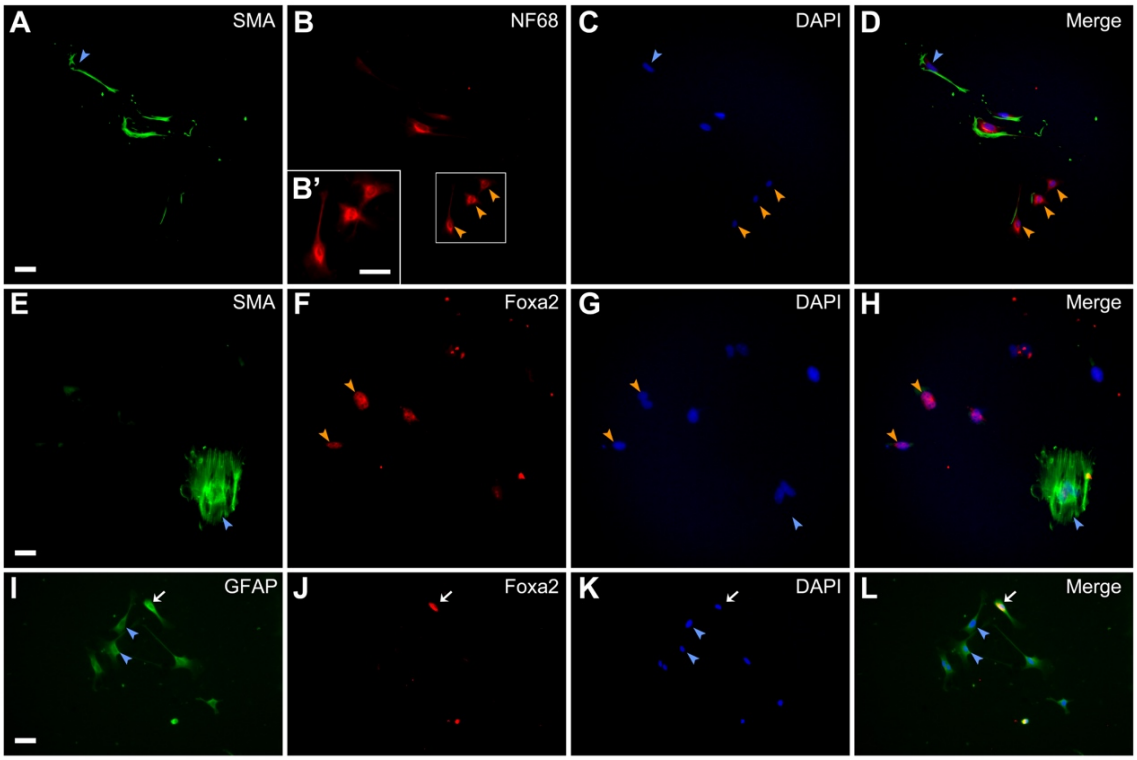


**Fig. 5**

**Developmental capacities of single DRG cells.**

E12 mouse DRG explants were cultured for 2 days and clonal culture analysis was subsequently performed in the presence of differentiation promoting factors for 5 days. Immunostaining using anti-SMA and anti-NF68, anti-SMA and anti-Foxa2, or anti-SMA and anti-GFAP was carried out on culture day 7. (A) Anti-SMA-positive cells. (B) Anti-NF68-positive cells in the same field as A. (C) DAPI nuclear staining of the same field as A. (D) Merged image of A-C. (E) Anti-SMA-positive cells. (F) Anti-Foxa2-positive cells in the same field as E. (G) DAPI nuclear staining of the same field as E. (H) Merged image of E-G. (I) Anti-GFAP-positive cells. (J) Anti-Foxa2-positive cells in the same field as I. (K) DAPI nuclear staining of the same field as I. (L) Merged image of I-K. B′

shows enlarged images of boxed region in B. Blue arrowheads indicate anti-SMA-positive cells (A,C,D,E,G, and H) or anti-GFAP positive cells (I,K, and L). Orange arrowheads indicate anti-NF68-positive cells (B-D) or anti-Foxa2-positive cells (F-H). White arrows of I-L indicate cells expressing both GFAP and Foxa2. Scale bars: 50 μm.

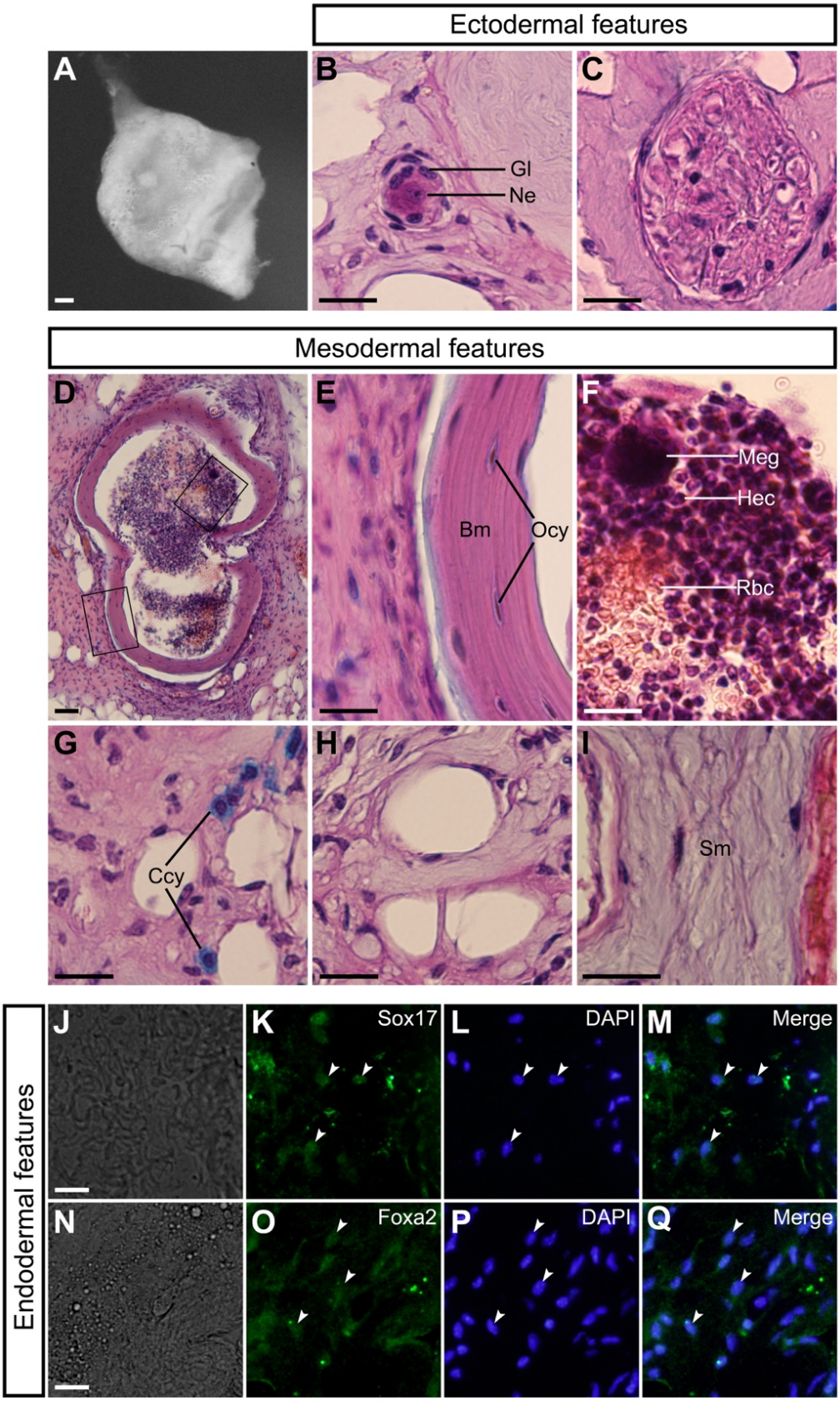
Ectodermal features
A
B
Gl
Ne
C
Mesodermal features
D
E
Bm
Ocy
F
Meg
Hec
Rbc
G
Ccy
H
I
Sm
Endodermal features
J
K
Sox17
L
DAPI
M
Merge
N
O
Foxa2
P
DAPI
Q
Merge

**Fig. 6**

***In vivo* developmental capacities of mouse embryonic DRG cells.**

(A) Teratomas were harvested at 2-3 months after injection of dissociated cells derived from E12 mouse DRGs. (B) Glia (Gl) and neuron (Ne). (C) Nerve fiber. (D) Bone and bone marrow. (E) Bone matrix (Bm) and osteocytes (Ocy) in enlarged images of one of the boxed regions in D. (F) Megakaryocyte (Meg), hematopoietic cells (Hec), and red blood cells (Rbc) in enlarged images of the boxed regions in D. (G) Chondrocytes (Ccy). (H) Adipocytes. (I) Smooth muscle (Sm). (J) Bright-field image. (K) Anti-Sox17-positive cells in the same field as J. (L) DAPI nuclear staining of the same field as J. (M) Merged image of K and L. White arrowheads in K-M indicate typical cells containing Sox17. (N) Bright-field image. (O) Anti-Foxa2-positive cells in the same field as N. (P) DAPI nuclear staining of the same field as N. (Q) Merged image of O and P. White arrowheads in O-Q indicate typical cells containing Foxa2. Scale bars: 200 μm in A; 50 μm in D; 20 μm in B,C,E-J, and N.

**Maintenance of expression of pluripotency-related transcription factors by addition of LIF/BMP2/FGF2**

Mouse embryonic and adult DRGs contain multipotent NCSCs (Paratore et al., 2002; Hjerling-Leffler et al., 2005; Nagoshi et al., 2008). It has been reported that Wnt/β-catenin activity plays important roles in NCSC formation in DRGs (Fig. 7; Kléber et al., 2004; Fujita et al., 2014). However, there is a loss of this activity in mouse DRGs around E12 (Fig. 7; Kléber et al., 2004). Therefore, different signal transduction pathways may participate in the maintenance of multipotency of NCSCs in DRGs after mouse E12, but little is known about their mechanisms. To unravel the mechanisms, we explored signaling molecules that promote the maintenance of multipotency of NCSCs in E12 mouse DRGs. Based on the findings of previous studies using mouse neural crest cells (Murphy et al., 1994; Fujita et al., 2014), mouse ES cells (Ying et al., 2003; Hao et al., 2006; Ogawa et al., 2006), and adult mouse brain neural stem progenitor cells (Kukekov et al., 1997), we focused on LIF, Wnt3a, BMP2, FGF2, and EGF (Fig. 7). The number of cells expressing both CHD7 and Sox10, which play essential roles in the formation of multipotent NCSCs in mice (Fujita et al., 2014), was counted on explant culture day 6. The percentage of these cells in a DRG cell colony (each colony was derived from a DRG explant) was highest in colonies cultured with the combination of LIF, BMP2, and FGF2 (Fig. 8). This result suggests that LIF/BMP2/FGF2 is the most effective in the maintenance of multipotency of NCSCs in mouse DRGs after E12.

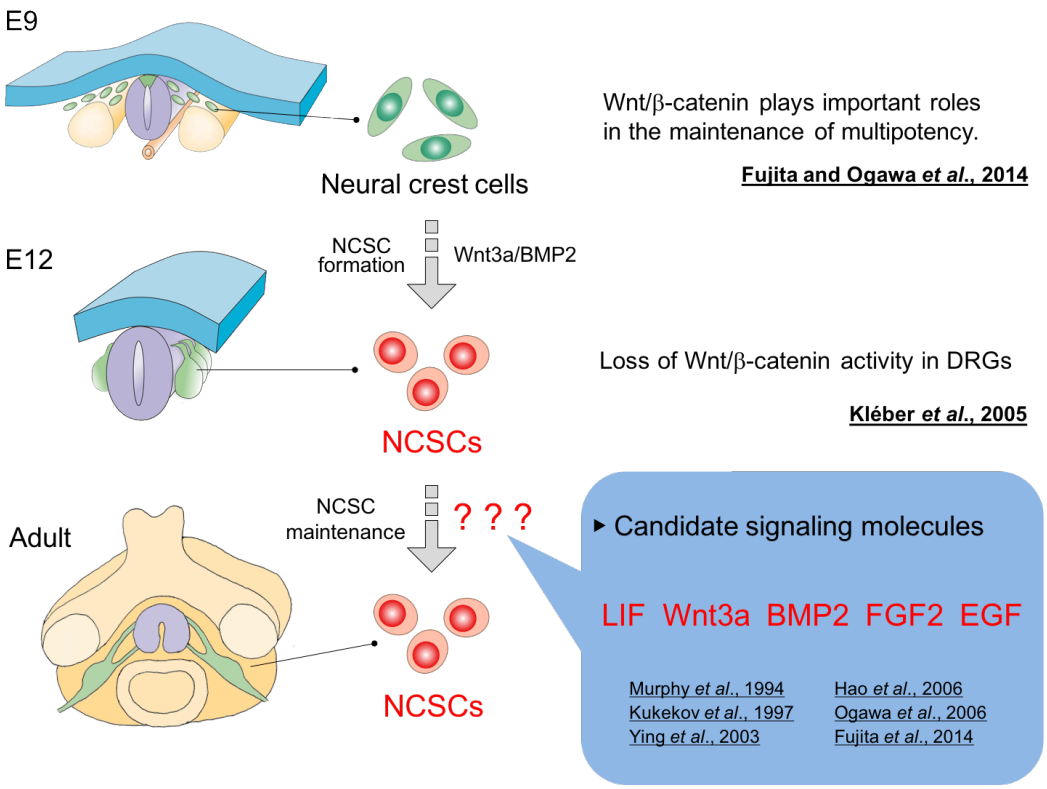


**Fig. 7**

**Roles of signaling molecules in formation of NCSCs and in maintenance of multipotency of NCSCs.**

Wnt3a/BMP2 signaling is involved in the maintenance of the multipotency of neural crest cells and in the formation of mouse NCSCs. Especially, Wnt/β-catenin activity plays important roles in NCSC formation in mouse embryonic DRGs. However, there is a loss of this activity in mouse DRGs around E12. Therefore, we focused on LIF, Wnt3a, BMP2, FGF2, and EGF, as candidates of signal molecules that are implicated in the maintenance of multipotency of NCSCs in DRGs after mouse E12.

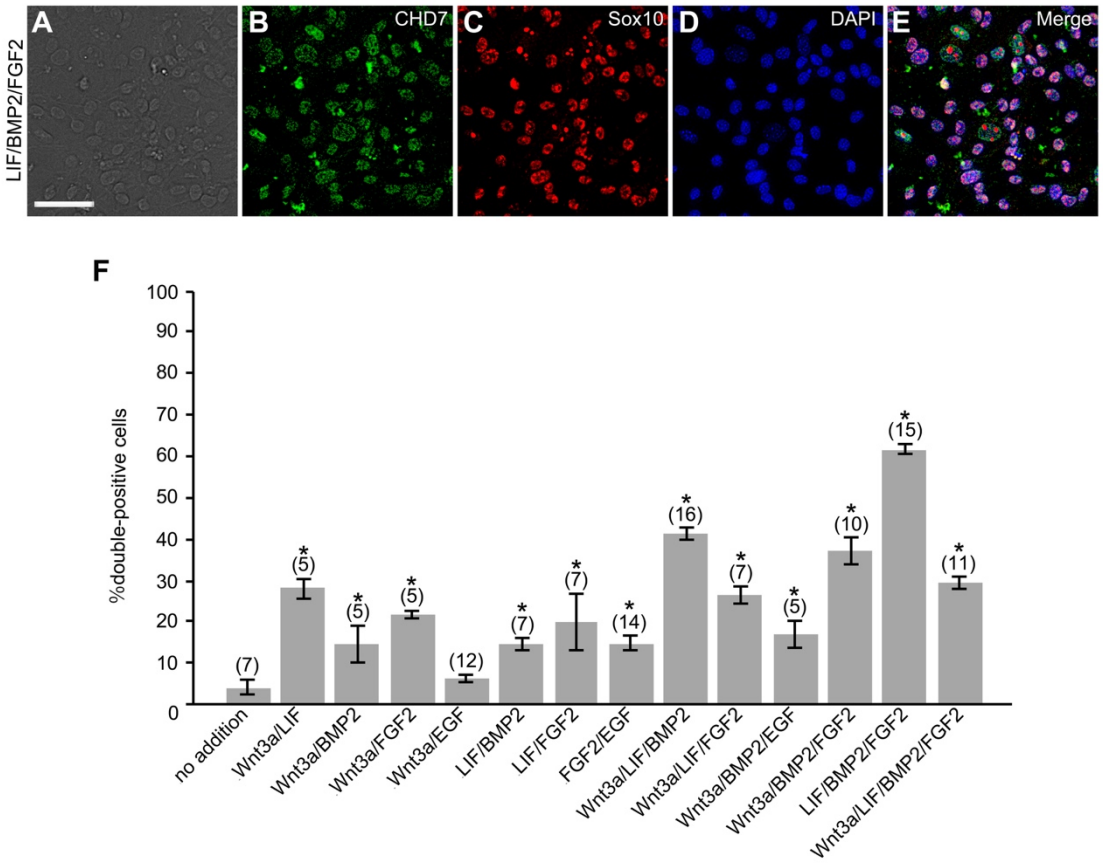


**Fig. 8**

**Signaling molecules that promote maintenance of NCSCs in mouse embryonic DRGs.**

E12 mouse DRG explants were exposed to signaling molecules for 6 days. Immunostaining was performed using anti-CHD7 or anti-Sox10 on culture day 6. (A) Bright-field image of a culture treated with LIF/BMP2/FGF2. (B) Anti-CHD7-positive cells in the same field as A. (C) Anti-Sox10-positive cells in the same field as A. (D) DAPI nuclear staining of the same field as A. (E) Merged image of B-D. (F) Percentage of cells expressing both CHD7 and Sox10 per DRG cell colony. **P*<0.05 (Student's *t*-test) compared to untreated

cultures. Data are expressed as mean±s.e.m. of separate counts of 5-16 colonies (the number in parentheses above each bar). Scale bar: 50 μm.

---

We examined the effects of LIF/BMP2/FGF2 on the expression of Oct4 in DRG cells in explant cultures. LIF/BMP2/FGF2 treatment promoted the expression of Oct4 (Fig. 9). The expression of Oct4 did not decrease over time in LIF/BMP2/FGF2-treated cultures (Fig. 9E). In addition, we investigated the effects of the combination of these signaling molecules on the expression of Sox2 and Nanog, which are pluripotency markers. When the number of cells expressing both Sox2 and Oct4 or both Nanog and Oct4 was counted on explant culture day 6, the treatment with LIF/BMP2/FGF2 significantly promoted the expression of Sox2 and Nanog (Fig. 10A-L). The number of anti-Sox2- or anti-Nanog-positive cells expressing Oct4 was also increased by LIF/BMP2/FGF2 treatment (Fig. 10M,N).

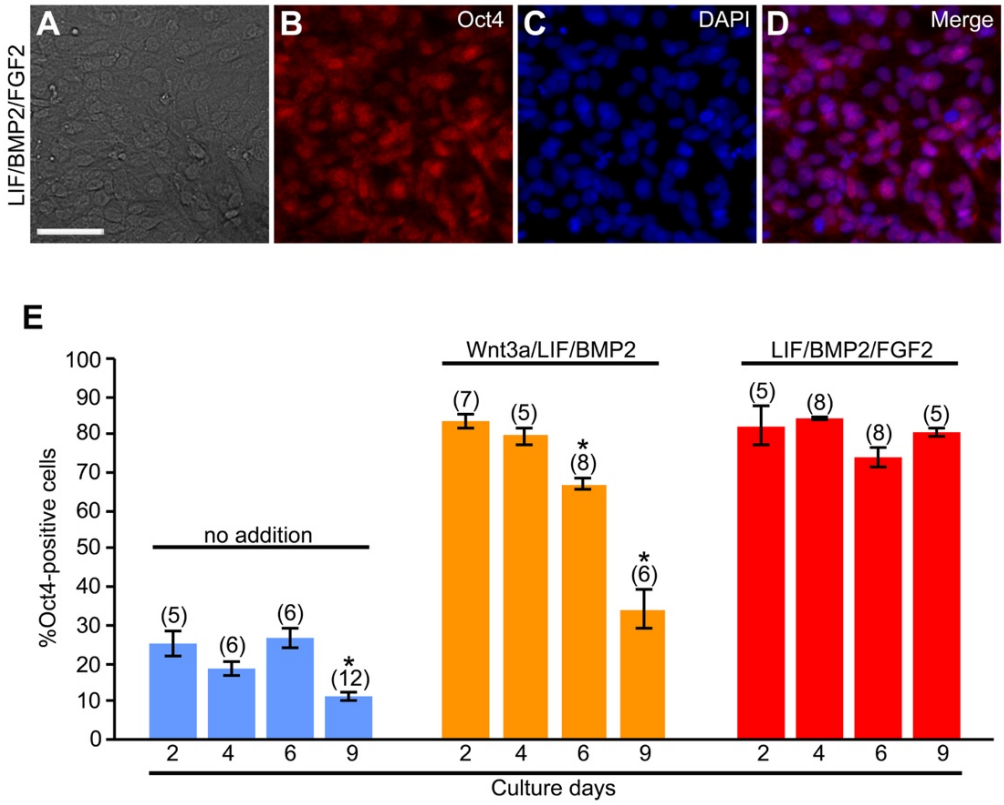


**Fig. 9**

**Effects of LIF/BMP2/FGF2 on expression of Oct4.**

E12 mouse DRG explants were exposed to signaling molecules for 2, 4, 6, or 9 days. Immunostaining was performed using anti-Oct4 on culture day 2, 4, 6, or 9. (A) Brightfield image of a culture treated with LIF/BMP2/FGF2 for 6 days. (B) Anti-Oct4-positive cells in the same field as A. (C) DAPI nuclear staining of the same field as A. (D) Merged image of B and C. (E) Percentage of cells expressing Oct4 per DRG cell colony. *$P$<0.05 (Student's $t$-test) compared to the cultures at 2 days under the respective conditions. Data are expressed as mean±s.e.m. of separate counts of 5-12 colonies (the number in parentheses above each bar). Scale bar: 50 μm.

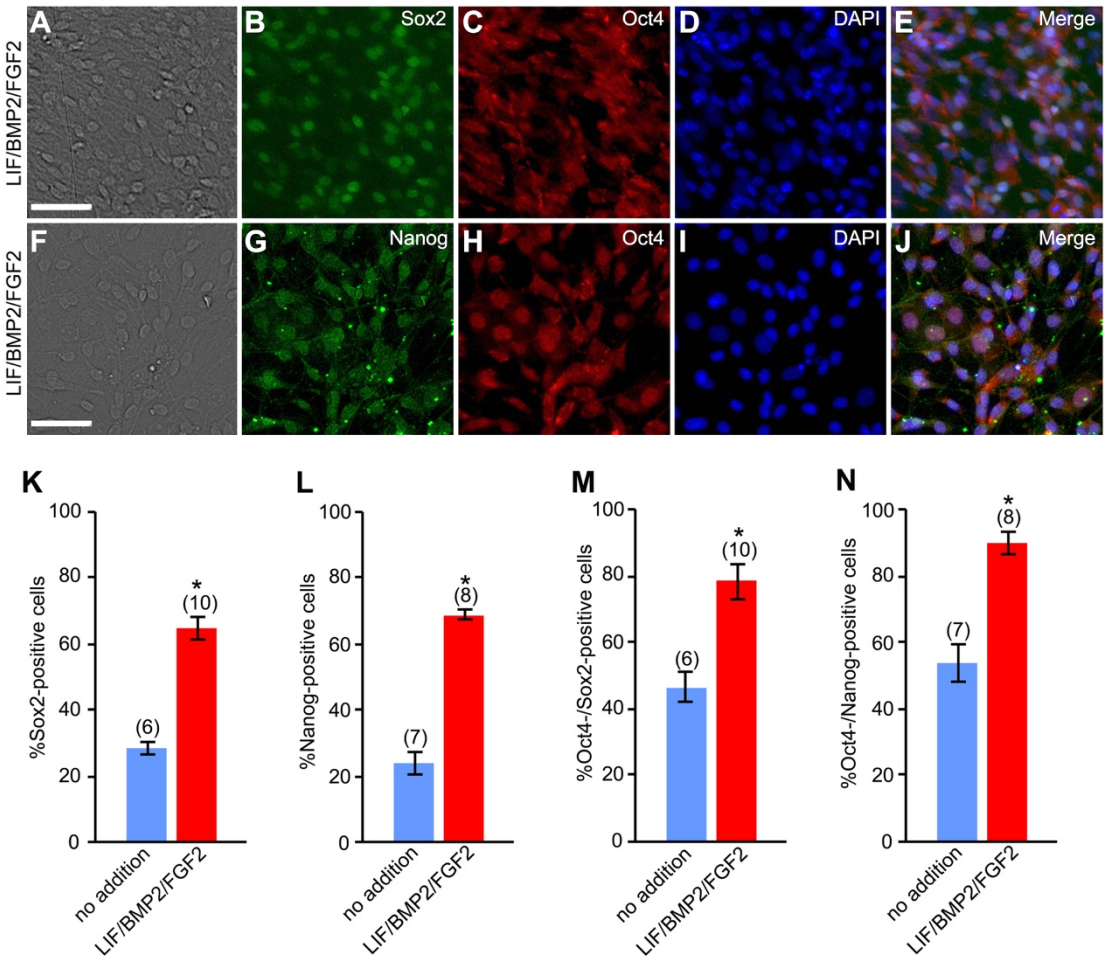


**Fig. 10**

**Effects of LIF/BMP2/FGF2 on expression of Sox2 and Nanog.**

E12 mouse DRG explants were cultured in medium containing LIF/BMP2/FGF2 for 6 days. Immunostaining was performed using anti-Oct4, anti-Sox2, or anti-Nanog on culture day 6. (A) Bright-field image of a culture treated with LIF/BMP2/FGF2. (B) Anti-Sox2-positive cells in the same field as A. (C) Anti-Oct4-positive cells in the same field as A. (D) DAPI nuclear staining of the same field as A. (E) Merged image of B-D. (F) Bright-field image of LIF/BMP2/FGF2-treated culture. (G) Anti-Nanog-positive cells in the same

field as F. (H) Anti-Oct4-positive cells in the same field as F. (I) DAPI nuclear staining of the same field as F. (J) Merged image of G-I. (K) Percentage of cells expressing Sox2 per DRG cell colony. (L) Percentage of cells expressing Nanog per DRG cell colony. (M) Percentage of cells expressing both Oct4 and Sox2 per total cells expressing Sox2 in a DRG cell colony. (N) Percentage of cells coexpressing Oct4 and Nanog per total cells expressing Nanog in a DRG cell colony. *$P$<0.05 (Student's $t$-test) compared to untreated cultures. Data are expressed as mean±s.e.m. of separate counts of 6-10 colonies (the number above the parentheses on each bar). Scale bars: 50 μm.

---

**Developmental capacities of mouse embryonic DRG cells treated with LIF/BMP2/FGF2**

LIF/BMP2/FGF2 treatment promoted the expression of pluripotency-related transcription factors in mouse embryonic DRG cells. Therefore, we examined the developmental potentials of DRG cells treated with LIF/BMP2/FGF2. DRG explants were cultured in medium containing LIF/BMP2/FGF2 during the first 6 days and subsequently exposed to various differentiation promoting factors (Fig. 11A). These cells differentiated into neurons in BMP4-treated cultures (Fig. 11B-E), into glia in FGF2-treated cultures (Fig. 11F-I), into smooth muscle cells in TGFβ-treated cultures (Fig. 11J-M), into chondrocytes in FGF2-treated cultures (Fig. 11N-Q), into anti-Sox17-positive endodermal cells in activin A-treated cultures (Fig. 11R-U), and into anti-

Foxa2-positive endodermal cells in activin A-treated cultures (Fig. 11V-Y). On the other hand, when DRG explants were cultured for 6 days under the control condition that did not contain LIF/BMP2/FGF2, the differentiation into neurons, glia, and chondrocytes was dramatically suppressed (Fig. 12).

We carried out clonal culture analysis to examine the developmental capacities of single cells derived from the DRG explants treated with LIF/BMP2/FGF2. We found clones containing both smooth muscle cells (Fig. 13A,D) and neurons (Fig. 13B,D) in BMP4-treated cultures. We also observed clones containing both smooth muscle cells (Fig. 13E,H) and endodermal cells expressing Foxa2 (Fig. 13F,H) in activin A-treated cultures. Clones containing cells which express both GFAP and Foxa2 (Fig. 13I,J,L) appeared in the presence of activin A and FGF2. However, no cells expressing Foxa2 only were observed under this condition.

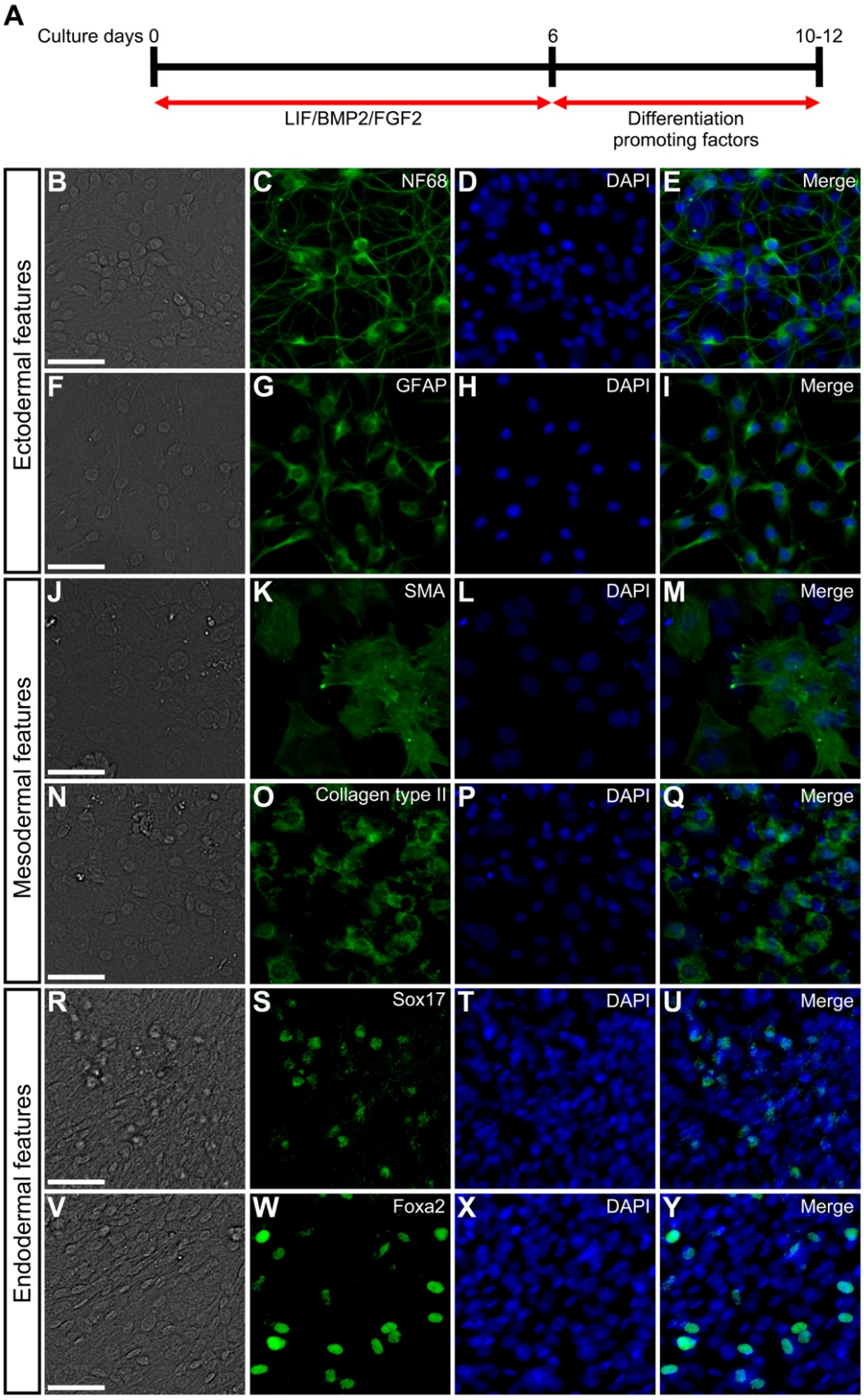
A
Culture days 0
6
10-12
LIF/BMP2/FGF2
Differentiation promoting factors
Ectodermal features
Mesodermal features
Endodermal features
B
C NF68
D DAPI
E Merge
F
G GFAP
H DAPI
I Merge
J
K SMA
L DAPI
M Merge
N
O Collagen type II
P DAPI
Q Merge
R
S Sox17
T DAPI
U Merge
V
W Foxa2
X DAPI
Y Merge

**Fig. 11**

**Developmental capacities of mouse embryonic DRG cells in explant cultures containing LIF/BMP2/FGF2.**

(A) E12 mouse DRG explants were cultured in medium containing LIF/BMP2/FGF2 during the first 6 days and subsequently exposed to differentiation promoting factors for 4 or 6 days. Immunostaining was performed using anti-NF68, anti-GFAP, anti-SMA, anti-Collagen type II, anti-Sox17, or anti-Foxa2 on culture day 10 or 12. (B) Bright-field image. (C) Anti-NF68-positive cells in the same field as B. (D) DAPI nuclear staining of the same field as B. (E) Merged image of C and D. (F) Bright-field image. (G) Anti-GFAP-positive cells in the same field as F. (H) DAPI nuclear staining of the same field as F. (I) Merged image of G and H. (J) Bright-field image. (K) Anti-SMA positive cells in the same field as J. (L) DAPI nuclear staining of the same field as J. (M) Merged image of K and L. (N) Bright-field image. (O) Anti-Collagen type II-positive cells in the same field as N. (P) DAPI nuclear staining of the same field as N. (Q) Merged image of O and P. (R) Bright-field image. (S) Anti-Sox17-positive cells in the same field as R. (T) DAPI nuclear staining of the same field as R. (U) Merged image of S and T. (V) Bright-field image. (W) Anti-Foxa2-positive cells in the same field as V. (X) DAPI nuclear staining of the same field as V. (Y) Merged image of Wand X. Scale bars: 50 μm.

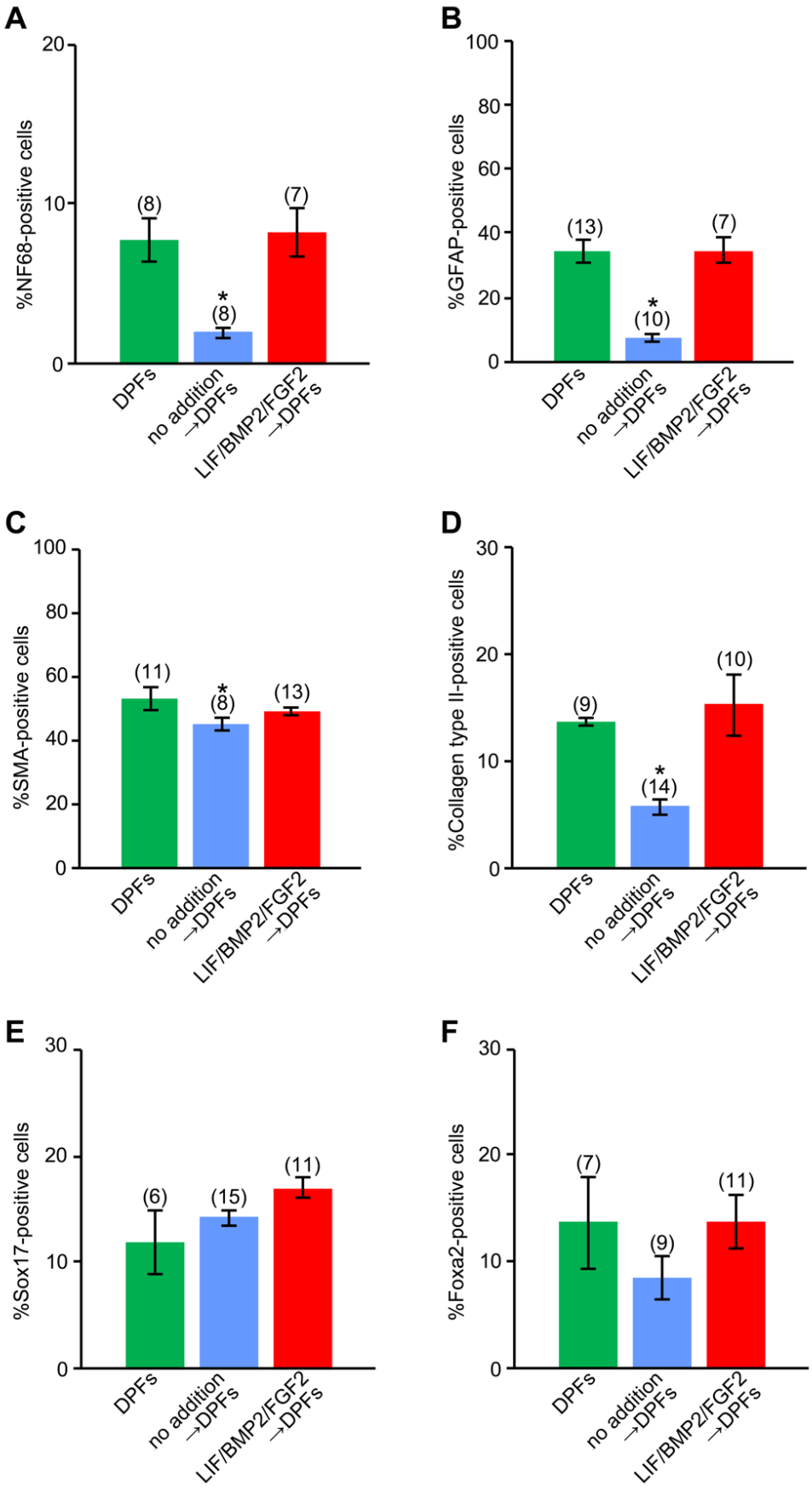
A
%NF68-positive cells
20
10
0
(8)
*
(8)
(7)
DPFs
no addition →DPFs
LIF/BMP2/FGF2 →DPFs
B
%GFAP-positive cells
100
80
60
40
20
0
(13)
*
(10)
(7)
DPFs
no addition →DPFs
LIF/BMP2/FGF2 →DPFs
C
%SMA-positive cells
100
80
60
40
20
0
(11)
*
(8)
(13)
DPFs
no addition →DPFs
LIF/BMP2/FGF2 →DPFs
D
%Collagen type II-positive cells
30
20
10
0
(9)
*
(14)
(10)
DPFs
no addition →DPFs
LIF/BMP2/FGF2 →DPFs
E
%Sox17-positive cells
30
20
10
0
(6)
(15)
(11)
DPFs
no addition →DPFs
LIF/BMP2/FGF2 →DPFs
F
%Foxa2-positive cells
30
20
10
0
(7)
(9)
(11)
DPFs
no addition →DPFs
LIF/BMP2/FGF2 →DPFs

**Fig. 12**

**Effects of LIF/BMP2/FGF2 on developmental capacities of mouse embryonic DRG cells.**

The DRG cells originated from E12 mouse DRG explants. (A) Percentage of cells expressing NF68 per DRG cell colony. (B) Percentage of cells expressing GFAP per DRG cell colony. (C) Percentage of cells expressing SMA per DRG cell colony. (D) Percentage of cells expressing Collagen type II per DRG cell colony. (E) Percentage of cells expressing Sox17 per DRG cell colony. (F) Percentage of cells expressing Foxa2 per DRG cell colony. *$P$<0.05 (Student's $t$-test) compared to DRG cell cultures treated with differentiation promoting factors from the first day in culture. Data are expressed as mean±s.e.m. of separate counts of 6-15 colonies (the number in parentheses above each bar). DPFs, differentiation promoting factors.

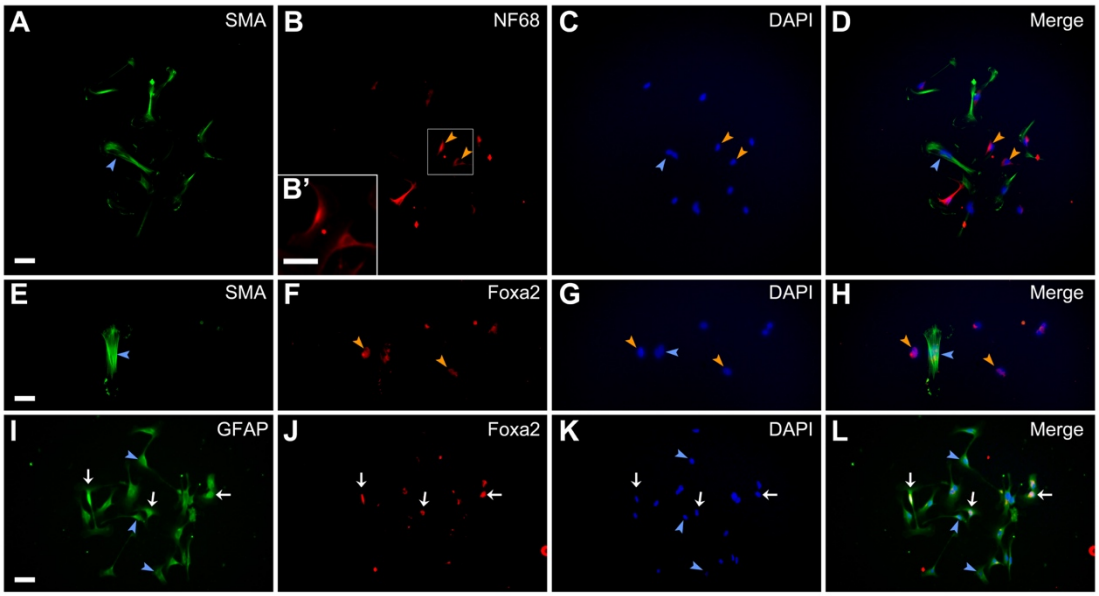


**Fig. 13**

**Developmental capacities of single cells derived from E12 mouse DRG explants treated with LIF/BMP2/FGF2.**

The DRG explants were cultured in the medium containing LIF/BMP2/FGF2 for 2 days and clonal culture analysis was subsequently performed in the presence of differentiation promoting factors for 5 days. Immunostaining using anti-SMA and anti-NF68, anti-SMA and anti-Foxa2, or anti-SMA and anti-GFAP was carried out on culture day 7. (A) Anti-SMA positive cells. (B) Anti-NF68-positive cells in the same field as A. B′ shows enlarged images of boxed region in B. (C) DAPI nuclear staining of the same field as A. (D) Merged image of A-C. (E) Anti-SMA-positive cells. (F) Anti-Foxa2-positive cells in the same field as E. (G) DAPI nuclear staining of the same field as E. (H) Merged image of E-G. (I) Anti-GFAP-positive cells. (J) Anti-Foxa2-positive cells in the same field as I. (K) DAPI nuclear staining of the same field as I.

(L) Merged image of I-K. Blue arrowheads indicate anti-SMA-positive cells (A,C,D,E,G, and H) or anti-GFAP-positive cells (I,K, and L). Orange arrowheads indicate anti-NF68-positive cells (B-D) or anti-Foxa2-positive cells (F-H). White arrows of I-L indicate cells expressing both GFAP and Foxa2. Scale bars: 50 μm.

---

We performed the teratoma formation assay using cells dissociated from the DRG explants cultured for 6 days in the presence of LIF/BMP2/FGF2, and found that teratomas were formed by injecting dissociated DRG cells treated with LIF/BMP2/FGF2 (Fig. 14A). The teratomas contained ectoderm-derived cell types (Fig. 14B,C), mesoderm-derived cell types (Fig. 14D-F), and endoderm-derived cell types (Fig. 14G). Endodermal cells expressing Sox17 (Fig. 14H-K) or Foxa2 (Fig. 14L-O) were observed. By contrast, no teratomas were formed by injecting cells dissociated from the DRG explants cultured for 6 days under the control condition.

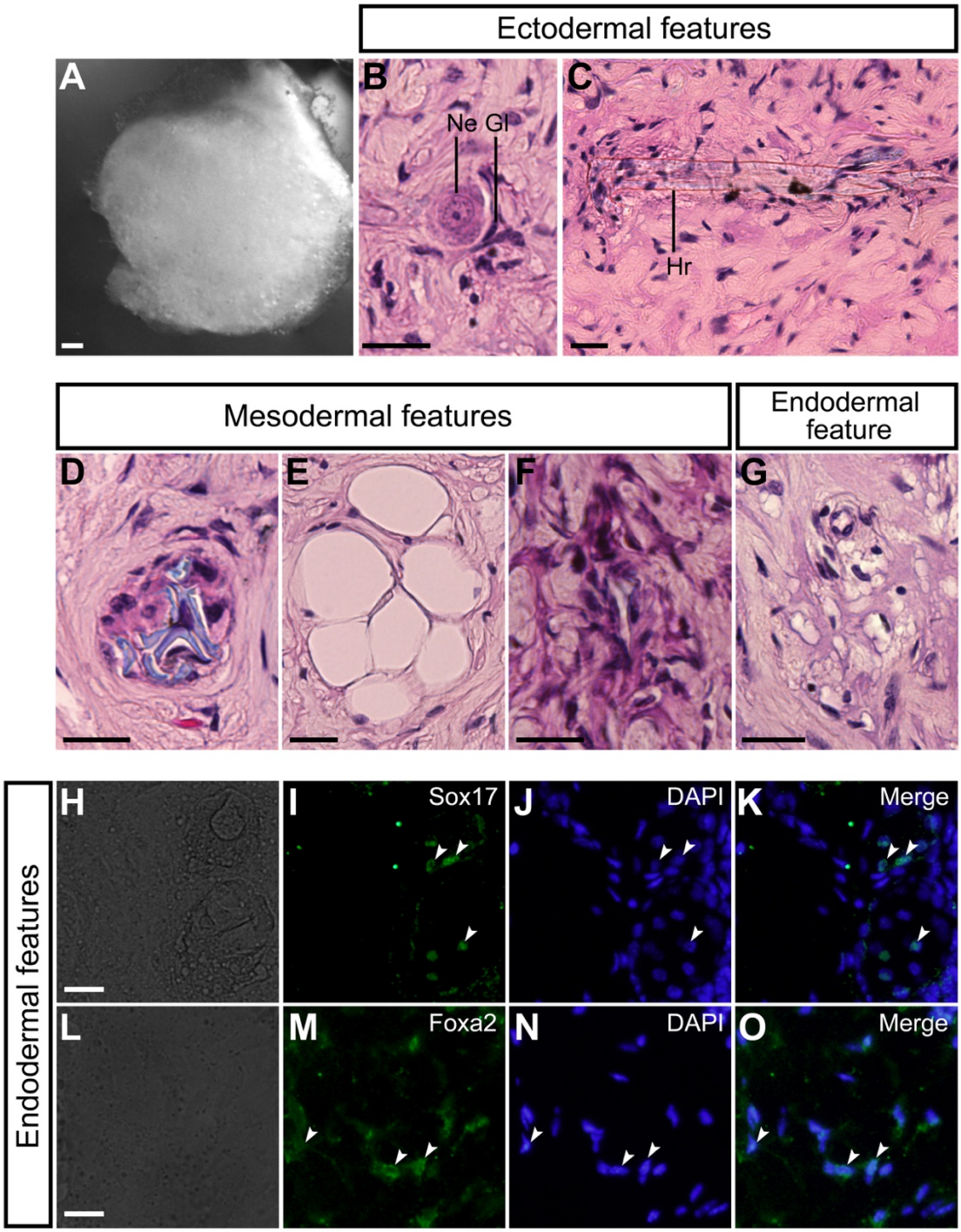


**Fig. 14**

***In vivo* developmental capacities of mouse embryonic DRG cells treated with LIF/BMP2/FGF2.**

(A) Teratomas were harvested at 2-3 months after injection of dissociated cells that had been derived from E12 mouse DRG explants cultured for 6 days in medium containing LIF/BMP2/FGF2. (B) Glia (Gl) and neuron (Ne). (C) Hair (Hr). (D) Cartilage. (E) Adipocytes. (F) Connective tissue. (G) Alveolar epithelium-like structure. (H) Bright-field image. (I) Anti-Sox17-positive cells in the same field as H. (J) DAPI nuclear staining of the same field as H. (K) Merged image of I and J. White arrowheads in I-K indicate typical cells containing Sox17. (L) Bright-field image. (M) Anti-Foxa2-positive cells in the same field as L. (N) DAPI nuclear staining of the same field as L. (O) Merged image of M and N. White arrowheads in M-O indicate typical cells containing Foxa2. Scale bars: 200 μm in A; 20 μm in B-H and L.

**Proliferation of Oct4-expressing DRG cells**

We then examined the proliferation of anti-Oct4-positive DRG cells in LIF/BMP2/FGF2-treated cultures. The number of cells expressing PCNA was counted on explant culture day 6. The percentage of anti-PCNA-positive proliferating cells per DRG cell colony was increased by treatment with LIF/BMP2/FGF2 (Fig. 15K). The proportion of anti-PCNA-positive cells per total Oct4-expressing cells was also increased by this treatment (Fig. 15A-E,L). DAPI nuclear staining showed that almost no cell death occurred in cultures treated with LIF/BMP2/FGF2. Therefore, we assessed apoptosis under the control and LIF/BMP2/FGF2-treated conditions. No significant difference of the proportion of apoptotic cell death was found between these conditions (Fig. 15M). No cells expressing both caspase-3 and Oct4 (Fig. 15F-J) were observed.

ES cells generate EB-like spheres in suspension cultures (Koike et al., 2005; Kurosawa, 2007). Therefore, we examined whether or not DRG cells form spheres in suspension culture. The DRG cells formed spheres both with and without LIF/BMP2/FGF2 treatment (Fig. 16B,C). However, the size of the spheres was significantly increased by the addition of LIF/BMP2/FGF2 (Fig. 16A).

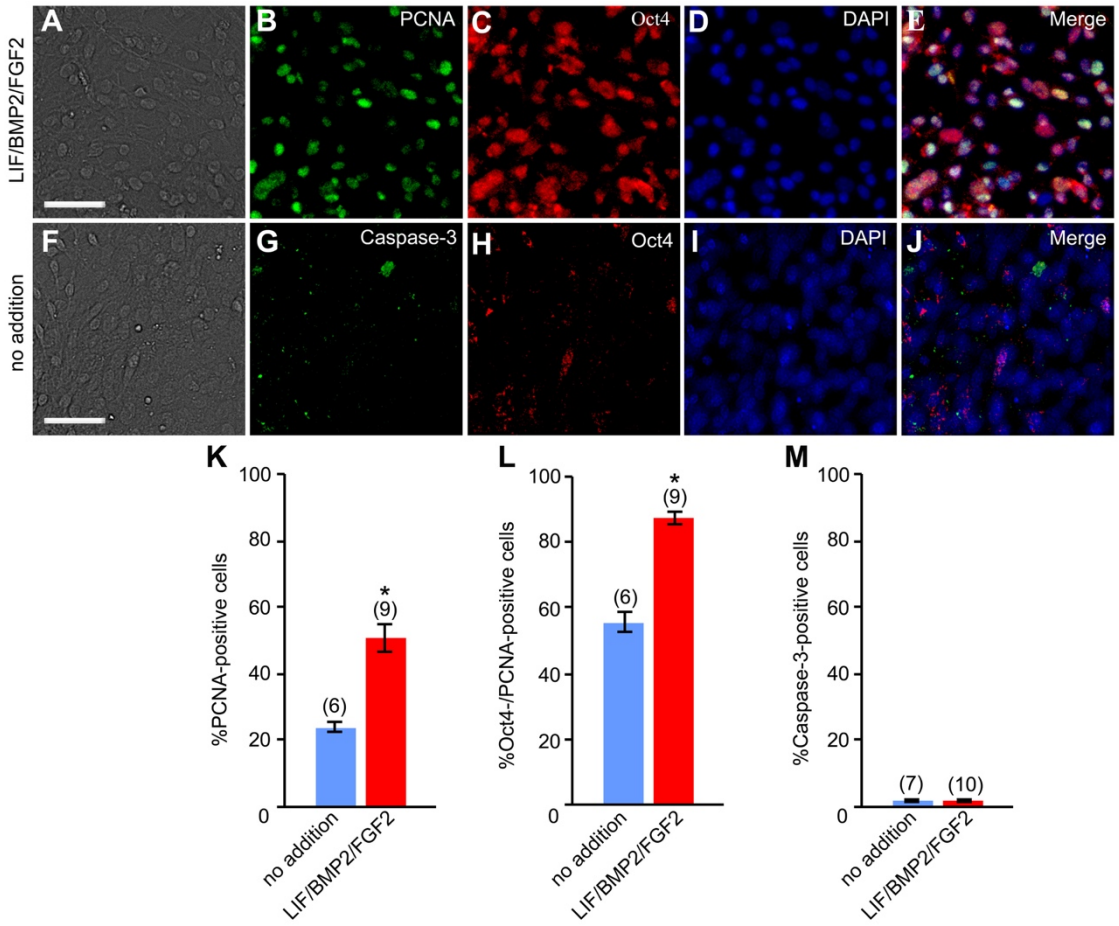


**Fig. 15**

**Effects of LIF/BMP2/FGF2 on proliferation of mouse embryonic DRG cells.**

E12 mouse DRG explants were cultured in medium containing LIF/BMP2/FGF2 for 6 days. Immunostaining was performed using anti-PCNA, anti-Oct4, and anti-Caspase-3 on culture day 6. (A) Bright-field image of a culture treated with LIF/BMP2/FGF2. (B) Anti-PCNA-positive cells in the same field as A. (C) Anti-Oct4-positive cells in the same field as A. (D) DAPI nuclear staining of the same field as A. (E) Merged image of B-D. (F) Bright-field image of the untreated culture. (G) Anti-Cacpase-3-positive cells in the same field as F. (H) Anti-Oct4-positive cells in the same field as F. (I) DAPI nuclear staining of

the same field as F. (J) Merged image of G-I. (K) Percentage of cells expressing PCNA per DRG cell colony. (L) Percentage of cells coexpressing PCNA and Oct4 per total cells expressing PCNA in a DRG cell colony. (M) Percentage of cells expressing Caspase-3 per DRG cell colony. *$P$<0.05 (Student's $t$-test) compared to untreated cultures. Data are expressed as mean±s.e.m. of separate counts of 6-10 colonies (the number in parentheses above each bar). Scale bars: 50 μm.

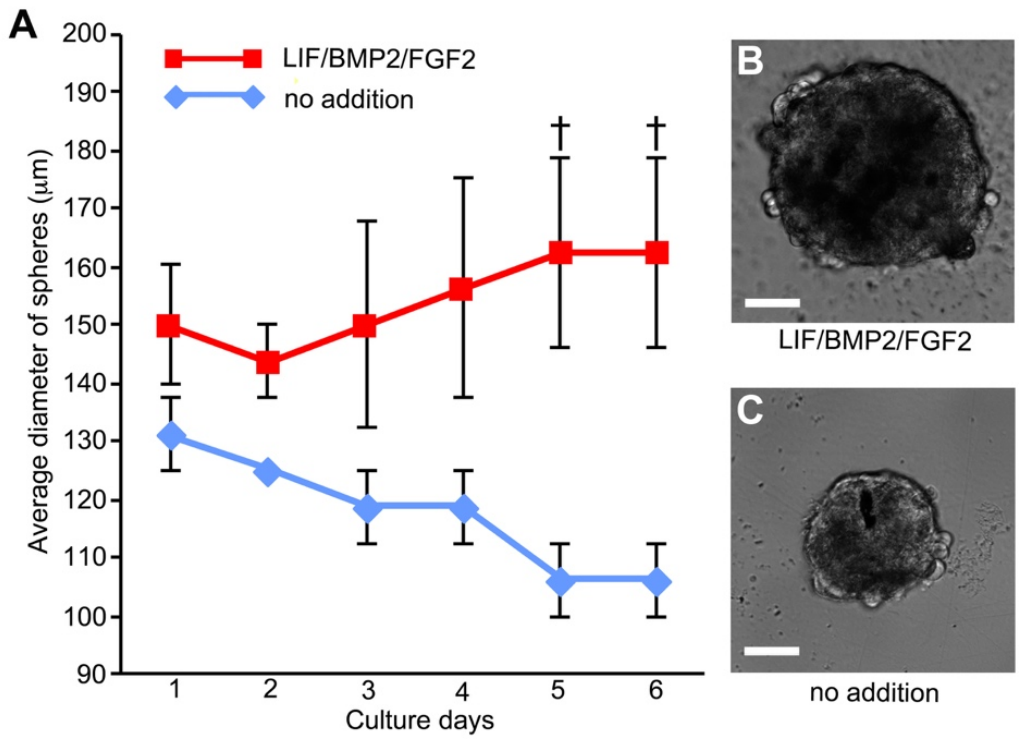


**Fig.16**

**Suspension cultures of mouse embryonic DRG cells.**

(A) Time course of average diameter of spheres in suspension cultures of dissociated cells derived from E12 mouse DRGs. Data are expressed as mean±s.e.m. of separate measurements of four spheres. †$P$<0.05 (Student's $t$-test) compared to untreated suspension cultures. (B) Bright-field image of a sphere cultured in the medium containing LIF/BMP2/FGF2 for 6 days. (C) Bright-field image of a sphere in the untreated culture at 6 days. Scale bars: 50 μm.

**Formation of PGCLCs from mouse embryonic DRG cells**

Mouse ES cells have been known to form PGCLCs expressing Blimp1 and Oct4 in LIF/BMP4-treated cultures (Kurimoto et al., 2015). Therefore, we investigated whether or not mouse embryonic DRG cells form PGCLCs. DRG explants were cultured on the time schedules shown in Fig. 17F. Since high concentrations of FBS block the formation of PGCLCs (Ohinata et al., 2009), we used Nu-serum instead of FBS and CEE. The culture condition containing 10% Nu-serum was the most effective in the formation of PGCLCs expressing both Blimp1 and Oct4 (Fig. 17A-E,G). There were no significant differences of PGCLC formation between the DRG explants treated with LIF/BMP4 only and those treated with LIF/BMP2/FGF2 and then LIF/BMP4 (Fig. 17G). These results indicate that LIF/BMP2/FGF2 maintains the capacity of PGCLCs formation of mouse embryonic DRG cells.

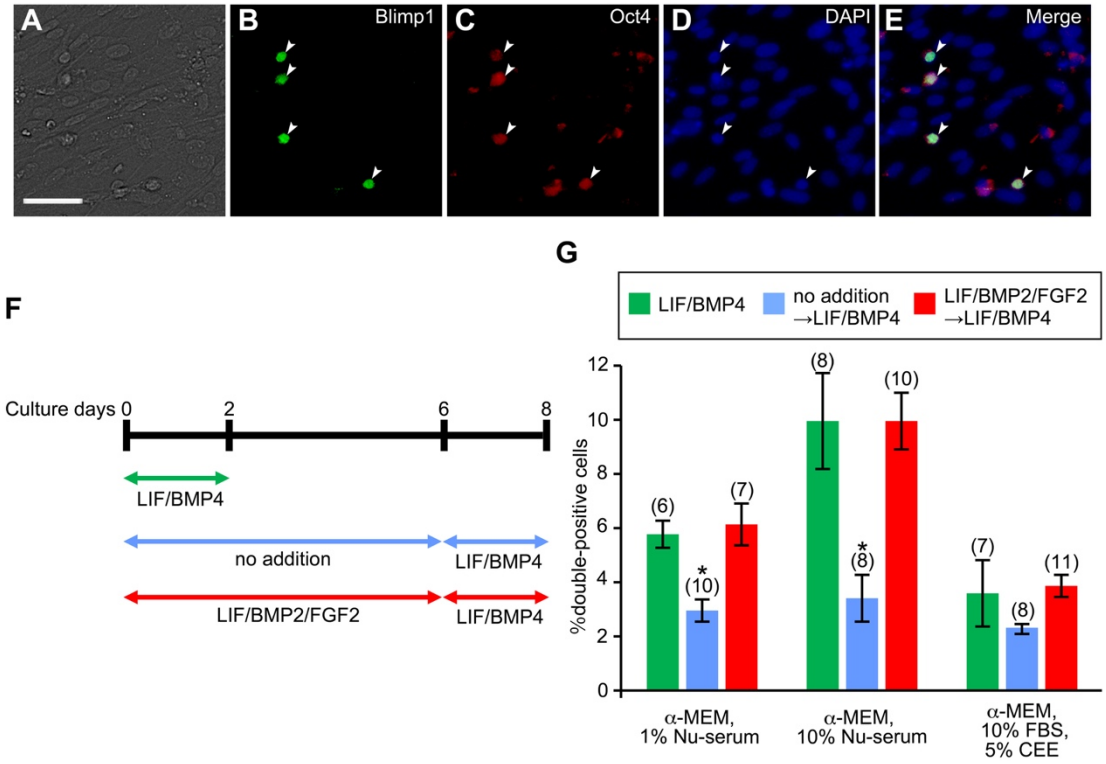


**Fig. 17**

**PGCLC formation by mouse embryonic DRG cells.**

E12 mouse DRG explants were cultured for 2 or 8 days. Immunostaining was performed using anti-Blimp1 and anti-Oct4 on culture day 2 or 8. (A) Bright-field image of a culture treated with LIF/BMP2/FGF2 during the first 6 days and subsequently exposed to 10% Nu-serum and LIF/BMP4 for 2 days. (B) Anti-Blimp1-positive cells in the same field as A. (C) Anti-Oct4-positive cells in the same field as A. (D) DAPI nuclear staining of the same field as A. (E) Merged image of B-D. White arrowheads in B-E indicate cells expressing both Blimp1 and Oct4. Scale bar: 50 μm. (F) Culture schedules of E12 mouse DRG explants for inducing the formation of PGCLCs. (G) Percentage of cells expressing both Blimp1 and Oct4 per DRG cell colony. *$P$<0.05 (Student's $t$-

test) compared to the cultures treated with LIF/ BMP4 for 2 days. Data are expressed as mean±s.e.m. of separate counts of 6-11 colonies (the number in parentheses above each bar).

---

Oct4, Sox2, and Nanog have been shown to interact with each other in the transcription regulatory network in mouse ES cells (Fig. 18A; Pan and Thomson, 2007; Chen et al., 2008). Therefore, we examined the interactions among Oct4, Sox2, and Nanog in cells dissociated from E12 mouse DRGs (Fig. 18B,C), in cells dissociated from the DRG explants cultured for 6 days under the control condition (Fig. 18D,E), and in cells dissociated from the DRG explants cultured for 6 days in the presence of LIF/BMP2/FGF2 (Fig. 18F,G) by μChIP- qPCR analysis. The interactions among these transcription factors in DRG cells dissociated from E12 mouse DRGs and in DRG cells treated with LIF/BMP2/FGF2 were similar to those in mouse ES cells (Fig. 18C,G). Concerning the regulatory network of Oct4, Sox2, and Nanog, thus, E12 mouse DRG cells have the similar network to that in mouse ES cells and LIF/BMP2/FGF2 helps to maintain this network.

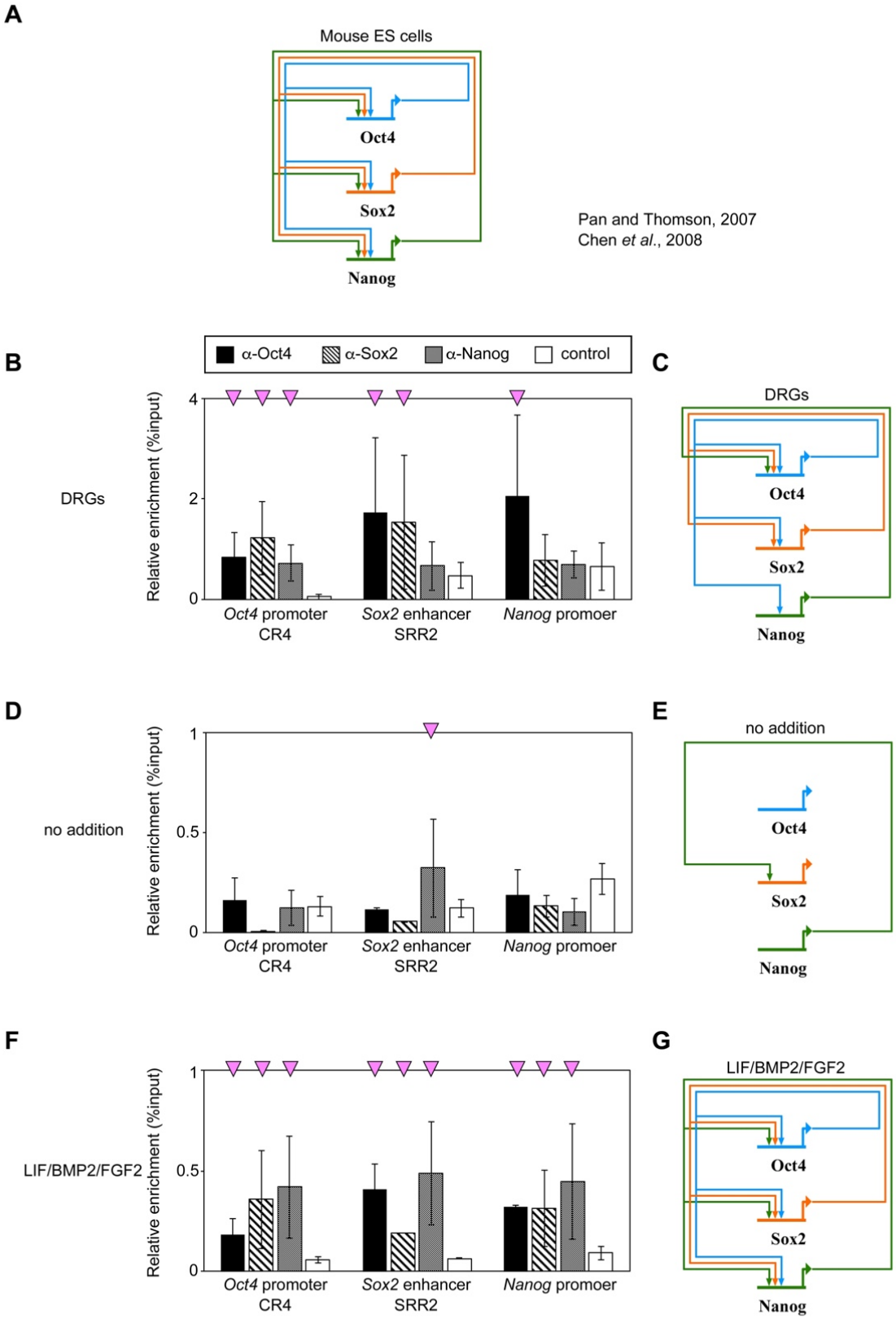
A
Mouse ES cells
Oct4
Sox2
Nanog
Pan and Thomson, 2007
Chen et al., 2008
B
α-Oct4
α-Sox2
α-Nanog
control
DRGs
Relative enrichment (%input)
4
2
0
Oct4 promoter CR4
Sox2 enhancer SRR2
Nanog promoer
C
DRGs
Oct4
Sox2
Nanog
D
no addition
Relative enrichment (%input)
1
0.5
0
Oct4 promoter CR4
Sox2 enhancer SRR2
Nanog promoer
E
no addition
Oct4
Sox2
Nanog
F
LIF/BMP2/FGF2
Relative enrichment (%input)
1
0.5
0
Oct4 promoter CR4
Sox2 enhancer SRR2
Nanog promoer
G
LIF/BMP2/FGF2
Oct4
Sox2
Nanog

**Fig. 18**

**Binding patterns of Oct4, Sox2, and Nanog to *Oct4* promoter CR4, *Sox2* enhancer SRR2, and *Nanog* promoter in mouse embryonic DRG cells.**

(A) Binding patterns of Oct4, Sox2, and Nanog to CR4, SRR2, and *Nanog* promoter in mouse ES cells. (B) μChIP-qPCR analysis of CR4, SRR2, and *Nanog* promoter performed using antibodies against Oct4, Sox2, and Nanog in E12 mouse DRGs. (C) Summary of binding patterns of Oct4, Sox2, and Nanog in E12 mouse DRGs. (D) μChIP-qPCR analysis of CR4, SRR2, and *Nanog* promoter performed using antibodies against Oct4, Sox2, and Nanog in DRG cells cultured for 6 days under the control condition. (E) Summary of binding patterns of Oct4, Sox2, and Nanog in DRG cells under the control condition. (F) μChIP-qPCR analysis of CR4, SRR2, and *Nanog* promoter performed using antibodies against Oct4, Sox2, and Nanog in DRG cells treated with LIF/BMP2/FGF2 for 6 days. (G) Summary of binding patterns of Oct4, Sox2, and Nanog in DRG cells treated with LIF/BMP2/FGF2. The DRG cells were derived from E12 mouse DRG explants. Pink triangles show the specific binding of Oct4, Sox2, or Nanog compared to control. The Y-axis represents percentage of co-immunoprecipitated DNA over input. Data are presented as mean±s.e.m. of 2 independent experiments carried out with duplicates.

**Relationship between NCSCs and PSCs**

Our data presented above suggest that mouse embryonic DRGs contain PSCs with characteristics similar to those of ES cells. Therefore, we examined whether or not PSCs were NCSCs. In mouse embryonic DRGs at E12, there were DRG cells that expressed Oct4 (Fig. 19B,E) and CHD7, a marker of multipotent NCSCs (Fig. 19C,E). Furthermore, cells expressing both Oct4 and CHD7 were observed in the DRGs (white arrowheads in Fig. 19B′-E′).

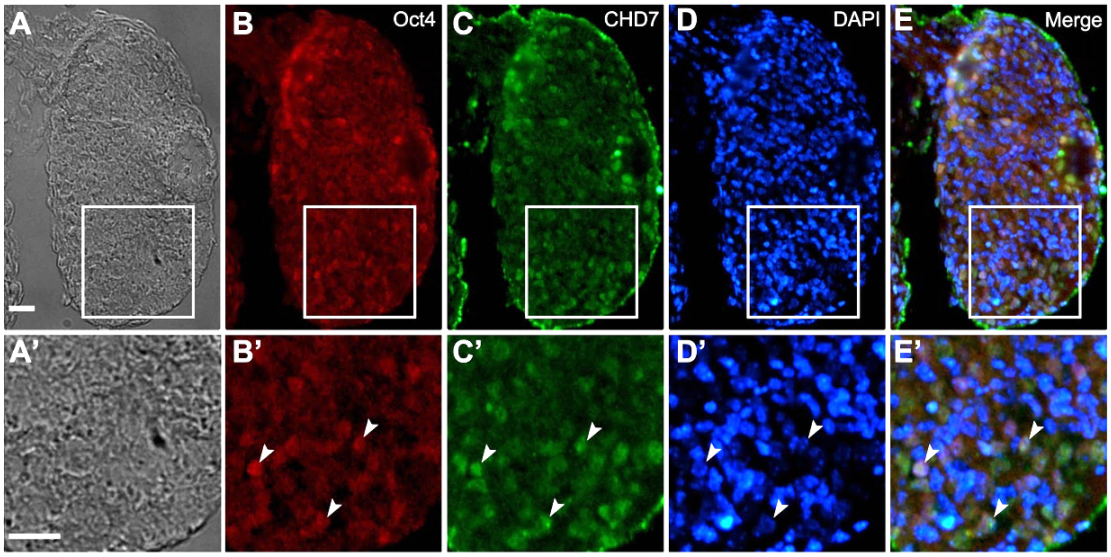


**Fig. 19**

**Coexpression of Oct4 and CHD7 in mouse embryonic DRGs.**

(A-E) Transverse sections of E12 mouse DRGs. The top, bottom, left, and right of each photograph correspond to the dorsal, ventral, proximal, and distal side of embryo, respectively. (A) Bright-field image. (B) Expression pattern of Oct4 in the same field as A. (C) Expression pattern of CHD7 in the same field

as A. (D) DAPI nuclear staining of the same field as A. (E) Merged image of B-D. A′-E′ show enlarged images of boxed regions in A-E. White arrowheads in B′-E′ indicate cells expressing both Oct4 and CHD7. Scale bars: 20 μm.

---

We explored whether the expression of Oct4 in mouse NCSCs is promoted by the addition of LIF/BMP2/FGF2. The percentage of cells expressing both Oct4 and CHD7 per DRG cell colony was drastically increased, and then never decreased over the culture period, by LIF/BMP2/FGF2 treatment (Fig. 20A-F). The proportion of cells expressing both Oct4 and CHD7 per total anti-CHD7-positive cells was also maintained over the culture period by the addition of LIF/BMP2/FGF2 (Fig. 20G).

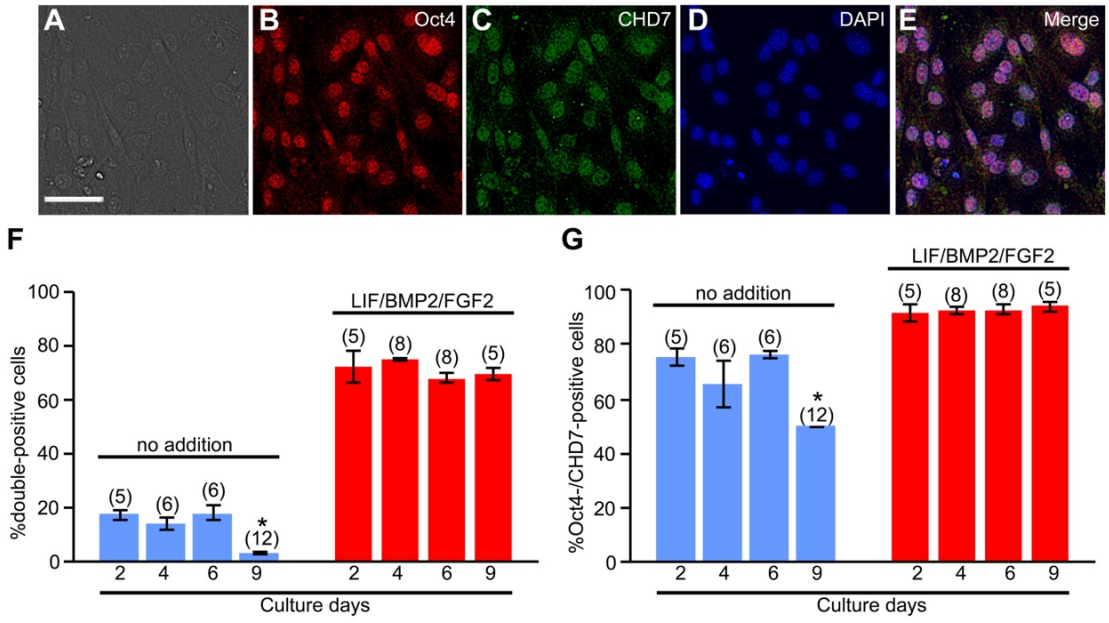


**Fig. 20**

***In vitro* coexpression of Oct4 and CHD7 in E12 mouse DRG explants on culture day 2, 4, 6, and 9.**

(A) Bright-field image of a culture treated with LIF/BMP2/FGF2 for 6 days. (B) Anti-Oct4-positive cells in the same field as A. (C) Anti-CHD7-positive cells in the same field as A. (D) DAPI nuclear staining of the same field as A. (E) Merged image of B-D. (F) Percentage of cells expressing both Oct4 and CHD7 per DRG cell colony. (G) Percentage of cells coexpressing Oct4 and CHD7 per total cells expressing CHD7 in a DRG cell colony. *$P$<0.05 (Student's $t$-test) compared to the cultures at 2 days under the respective conditions. Data are expressed as mean±s.e.m. of separate counts of 5-12 colonies (the number in parentheses above each bar). Scale bar: 50 μm.

---

We analyzed the regulatory interactions between pluripotency-related transcription factors, Oct4, Sox2, and Nanog, and the factors that characterize mouse NCSCs, CHD7 and Sox10. Mouse embryonic DRG cells in explant cultures were treated with expression vectors and siRNAs, as shown in Fig. 21A. Whereas the expression of Sox10 and Oct4 was promoted by treatment with the WT CHD7 expression vector (Fig. 21C,F), their expression was significantly suppressed by the DN CHD7 expression vector or *CHD7* siRNA in the presence of LIF/BMP2/FGF2 (Fig. 21C,F). The expression of CHD7 and Sox10 was suppressed by *Oct4*, *Sox2*, and *Nanog* siRNA in the presence of LIF/BMP2/FGF2 (Fig. 21B,C,E). Coexpression of CHD7 and Sox10 or of CHD7 and Oct4 was affected by these expression vectors and siRNAs (Fig. 21D,G). Thus, pluripotency-related transcription factors have regulatory interactions with the factors that characterize mouse NCSCs. When the DN CHD7

expression vectors were added, the number of anti-CHD7-positive cells increased (Fig. 21B,E), indicating that the anti-CHD7 antibody used in this study recognized the mutant CHD7, probably due to the fact that the mutation in this protein changed only lysine 998 in the ATPase domain of CHD7 to arginine.

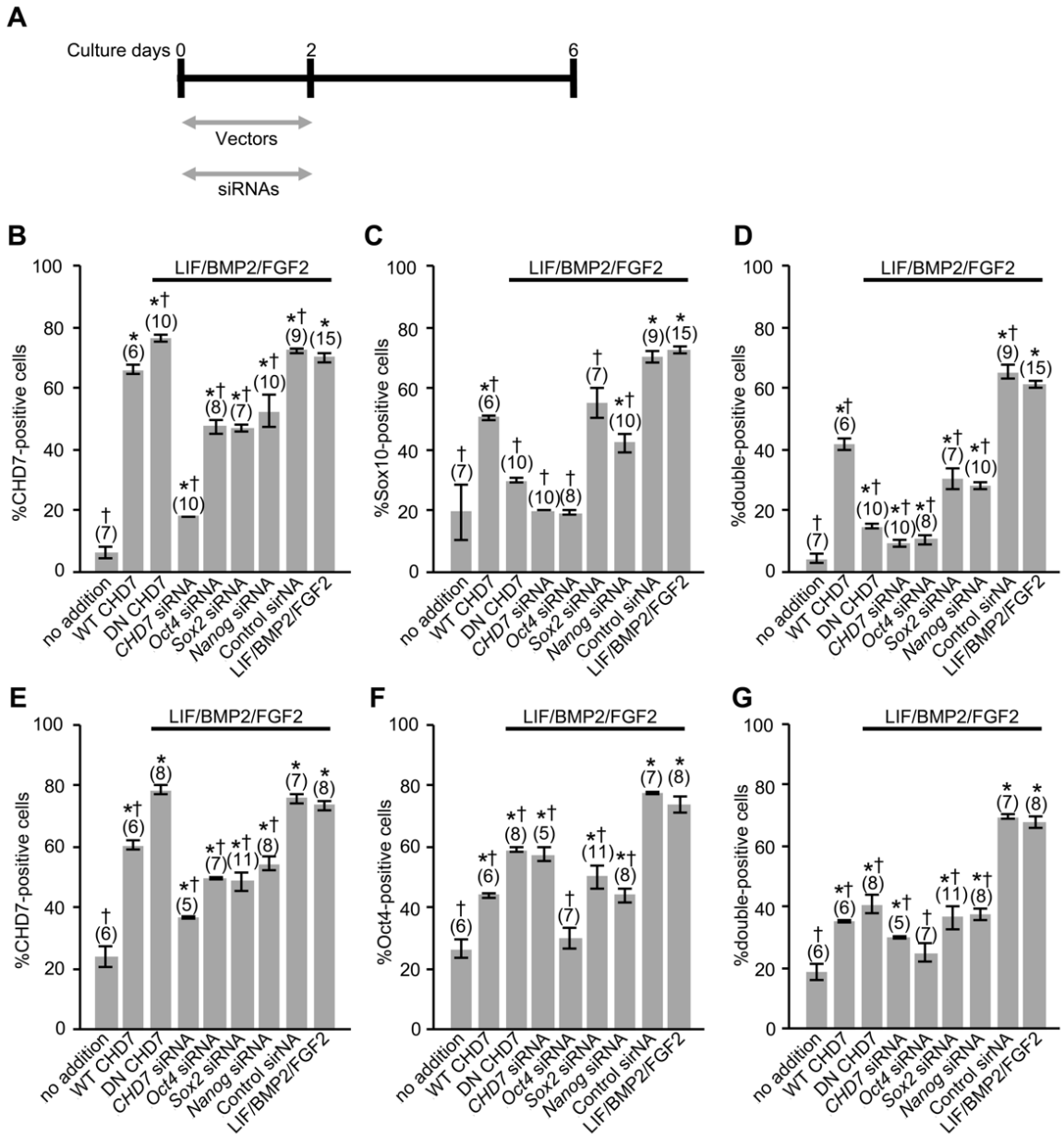

**Fig. 21**

**Effects of WT CHD7 or DN CHD7 expression vectors and of *CHD7*, *Oct4*, *Sox2*, or *Nanog* siRNAs on CHD7, Sox10, or Oct4 expression.**

(A) E12 mouse DRG explants were exposed to LIF/BMP2/FGF2 for 6 days. Each expression vector or siRNA was applied from day 0 to day 2 in culture. (B) Percentage of cells expressing CHD7 per DRG cell colony. (C) Percentage of cells expressing Sox10 per DRG cell colony. (D) Percentage of cells expressing both CHD7 and Sox10 per DRG cell colony. (E) Percentage of cells expressing CHD7 per DRG cell colony. (F) Percentage of cells expressing Oct4 per DRG cell colony. (G) Percentage of cells expressing both CHD7 and Oct4 per DRG cell colony. *$P$<0.05 (Student's $t$-test) compared to untreated cultures. †$P$<0.05 (Student's $t$-test) compared to LIF/BMP2/FGF2-treated cultures. Data are expressed as mean±s.e.m. of separate counts of 5-15 colonies (the number in parentheses above each bar).

# DISCUSSION

In the present study, we showed that mouse embryonic DRGs contain cells that express pluripotency-related transcription factors Oct4, Sox2, and Nanog. It has been reported that Oct4 (Nichols et al., 1998; Niwa et al., 2000), Sox2 (Avilion et al., 2003; Masui et al., 2007), and Nanog (Chambers et al., 2003; Mitsui et al., 2003) function in the maintenance of pluripotency in both early mouse embryonic pluripotent cells and ES cells. The DRGs expressed SSEA1 and showed alkaline phosphatase activity, which have been known to be pluripotency markers in mouse ES and iPS cells (Wobus et al., 1984; Cui et al., 2004; Takahashi and Yamanaka, 2006). In addition, we suggested here that DRG cells differentiated into ectoderm-, mesoderm-, and endoderm-derived cell types in explant cultures. In clonal cultures, we also found clones containing both ectoderm (neurons)- and mesoderm (smooth muscle cells)-derived cell types, both endodermal cells (Foxa2-expressing cells) and smooth muscle cells, or cells expressing both ectoderm (GFAP)- and endoderm (Foxa2)-derived features. These data suggest that some of the single DRG cells have ability to differentiate into cells which originate from three germ layers.

The DRG cells formed teratomas that contained ectoderm-, mesoderm-, and endoderm-derived cell types, like the teratomas formed by ES cells (Thomson et al., 1998) and by iPS cells (Takahashi and Yamanaka, 2006). The DRG cells also had sphere-forming capacity, as do ES cells (Desbaillets et al., 2000; Itskovitz-Eldor et al.,

2000) and iPS cells (Takahashi and Yamanaka, 2006). Furthermore, the DRG cells formed PGCLCs. This feature is also similar to that of ES cells (Hübner et al., 2003; Toyooka et al., 2003; Hayashi and Saitou, 2013) and iPS cells (Hayashi and Saitou, 2013). These data suggest the possibility that mouse embryonic DRGs contain PSCs with characteristics like those of ES cells and iPS cells.

Mouse embryonic DRGs cells formed teratomas containing bone marrow, in which megakaryocytes, hematopoietic cells, and red blood cells were observed. It has been reported that iPS cells form hematopoietic stem cells through teratoma formation (Suzuki et al., 2013). DRG cells may also have the capacity to form hematopoietic stem cells.

It has been shown that mouse embryonic and adult DRGs contain multipotent NCSCs (Paratore et al., 2002; Hjerling-Leffler et al., 2005; Nagoshi et al., 2008), and that Wnt/BMP signaling plays important roles in the formation of NCSCs (Kléber et al., 2004; Fujita et al., 2014). We suggested that the Wnt/β-catenin pathway is essential in this process (Fujita et al., 2014). However, Wnt/β-catenin activity disappears in mouse DRGs around E12 (Kléber et al., 2004). Thus, different signaling molecules may participate in the maintenance of multipotency of NCSCs in mouse DRGs. The present study showed that LIF/BMP2/FGF2 was the most effective tested combination of factors for the maintenance of multipotency of NCSCs in mouse DRGs at E12. These data imply that Wnt/BMP signaling works for the formation of NCSCs and LIF/BMP2/FGF2 signaling is involved in the maintenance of multipotency of NCSCs during mouse DRG development. While LIF maintains the pluripotency of mouse ES

cells, BMP2/4 and FGF play supportive roles in the maintenance of their pluripotency (Ying et al., 2003; Niwa et al., 2009; Tanaka et al., 2011). FGF2 has been implicated in the maintenance of pluripotency of human ES cells (Vallier et al., 2005; Levenstein et al., 2006). Therefore, we analyzed the effects of LIF/BMP2/FGF2 on the maintenance of pluripotency of PSCs in mouse embryonic DRGs. The addition of LIF/BMP2/FGF2 maintained the expression of Oct4, Sox2, and Nanog. The DRG cells sustained the capacities to differentiate into ectoderm-, mesoderm-, and endoderm-derived cell types *in vitro* and *in vivo*, when the cells were treated with LIF/BMP2/FGF2. The DRG cells treated with LIF/BMP2/FGF2 formed spheres and PGCLCs. These findings suggest that LIF/BMP2/FGF2 participates not only in the maintenance of multipotency of NCSCs, but also in the maintenance of pluripotency of PSCs in mouse embryonic DRGs (Fig. 22).

LIF/BMP2/FGF2 promoted cell proliferation of the DRG cells in both explant and suspension cultures. LIF/BMP2/FGF2 treatment stimulated the proliferation of the DRG cells expressing Oct4. The combination of these signaling molecules may promote the proliferation of PSCs as well as the maintenance of pluripotency of PSCs in mouse embryonic DRGs (Fig. 22).

Mouse and rat DRG cells have been shown to express LIF, BMP2, and FGF2 (Murphy et al., 1993, 1994; Farkas et al., 1999). The expression of receptors for these signaling molecules in DRGs has also been reported (Bengtsson et al., 1998; Walshe and Mason, 2000; Zhang et al., 2007). LIF/BMP2/FGF2 signaling may play important roles in the maintenance of pluripotency of PSCs in mouse embryonic DRGs *in vivo*.

Since LIF/BMP2/FGF2 was involved both in the maintenance of the expression of pluripotency-related transcription factors (Oct4, Sox2, and Nanog) and in the maintenance of the expression of factors that characterize mouse NCSCs (CHD7 and Sox10), we analyzed the relationship between pluripotency-related transcription factors and the factors that characterize mouse NCSCs in mouse embryonic DRGs. DRG cells expressing both Oct4 and CHD7 were observed *in vivo* and *in vitro*. The number of these cells *in vitro* was dramatically increased by LIF/BMP2/FGF2 treatment. Furthermore, the expression of Oct4 was suppressed by inhibiting the expression of CHD7 and the expression of CHD7 and Sox10 was repressed by *Oct4*, *Sox2*, and *Nanog* siRNA in the presence of LIF/BMP2/FGF2. These findings support the possibility that pluripotency-related transcription factors and factors that characterize mouse NCSCs were mutually regulated by each other in mouse embryonic DRGs. Thus, PSCs in mouse embryonic DRGs may be NCSCs in the DRGs. It has been shown that CHD7 binds to enhancer elements of *Oct4*, *Sox2*, and *Nanog* in mouse ES cells (Schnetz et al., 2010) and these cells express Sox10, although at a low level compared with that in neural crest cells (Hagiwara et al., 2014). Taken together, all these findings support the notion that NCSCs in mouse embryonic DRGs may have equivalent developmental potential to PSCs such as ES cells and iPS cells (Fig. 22). Thus, there may exist PSCs until much later developmental stages than those thought conventionally.

The method for isolation of mouse DRGs used in this study has been used in other studies (Moore et al., 2008; Chen 2014) to isolate rodent DRGs. However, we

cannot exclude the possibility that the isolated DRGs may contain non-DRG cells derived from surrounding tissues. Therefore, we consider that doing similar experiment to this study using other methods to isolate NCSCs, such as flow cytometry using p75 antibodies (Morrison et al.,1999), P0-Cre / Floxed-EGFP mice (Nagoshi et al., 2008), Wnt1-Cre / Floxed-EGFP mice (Nagoshi et al., 2008), or Sox10-IRES-Venus mice (Motohashi et al., 2014) is important for elucidating the property of NCSCs. In addition, it is necessary to exclude the possibility to contain non-neural crest-derived cells by using mice which have reporter genes that specifically express in neural crest-derived cells (Nagoshi et al., 2008; Motohashi et al., 2014) in clonal culture analysis and teratoma formation assay. Furthermore, these reporter containing mice are useful for confirming that tissues in teratoma originate from DRG cells injected.

Buitrago-Delgado et al. (2015) have reported that *Xenopus* neural crest cells differentiate into endodermal cells by activin treatment *in vitro*. In present study, it was suggested that mouse embryonic DRG cells differentiated into endodermal cells by activin treatment. However, there have been no reports that neural crest cells form endodermal tissues in normal development (Teillet et al., 1987; Shakhova and Sommer 2010; Mayor et al., 2013; Baggiolini et al., 2015). It is conceivable that this behavior of neural crest cells in normal development may be due to not encountering environmental factors that cause differentiation into endodermal cells in the developmental process. However, it may be necessary to examine whether or not neural crest cells indeed participate in the formation of endodermal cells *in vivo*.

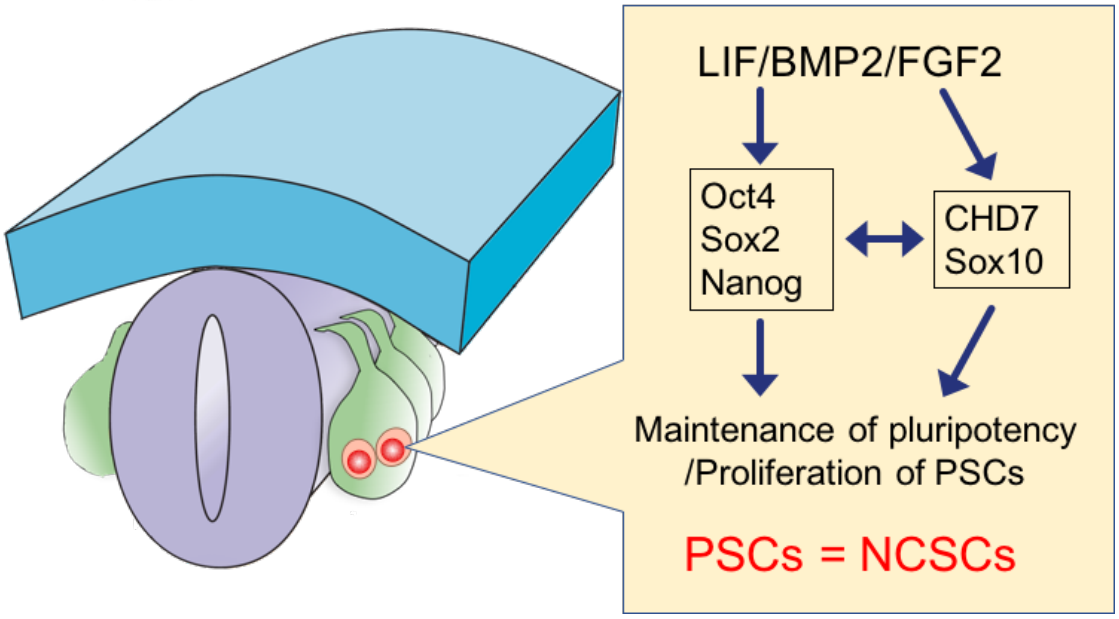


**Fig. 22**

**Summary for the present study.**

E12 mouse DRGs contain PSCs. LIF/BMP2/FGF2 is effective not only in maintenance of the expression of CHD7 and Sox10, but also in maintenance of the expression of Oct4, Sox2, and Nanog. Furthermore, the expression of pluripotency-related transcription factors in the DRG cells is regulated by CHD7 and Sox10, and vice versa. These data support the possibility that PSCs in mouse embryonic DRGs are NCSCs and suggest that pluripotency at the early stage of mouse embryonic development is inherited by mouse NCSCs.

## CONCLUSION

1. We examined the expression of pluripotency-related transcription factors (Oct4, Sox2, and Nanog) and SSEA1 and the activity of alkaline phosphatase in E12 mouse DRGs. Cells expressing pluripotency-related transcription factors and/or SSEA1 and showing alkaline phosphatase activity were found in mouse embryonic DRGs. Furthermore, we investigated the developmental potentials of the DRG cells *in vitro*. These cells differentiated into neurons, glia, chondrocytes, smooth muscle cells, and endodermal cells that express Sox17 or Foxa2. We also performed teratoma formation assay to assess *in vivo* developmental capacity of the DRG cells. The teratomas contained ectoderm-derived cell types, mesoderm-derived cell types, and endodermal cells. Mouse embryonic DRG cells formed PGCLCs and EB-like spheres. These data suggest the possibility that E12 mouse DRGs contain PSCs.

2. We examined what culture conditions are essential for the maintenance of NCSCs and PSCs in E12 mouse DRGs. We showed that LIF/BMP2/FGF2 was the most effective in the maintenance of multipotency of NCSCs in the DRGs. LIF/BMP2/FGF2 promoted the expression of Oct4, Sox2, and Nanog. Furthermore, it was observed that the DRG cells sustained the capacities to differentiate into ectoderm-, mesoderm-, and endoderm-derived cell types *in vitro*

and *in vivo*, when the cells were treated with LIF/BMP2/FGF2. These cells treated with LIF/BMP2/FGF2 also formed EB-like spheres and PGCLCs. Therefore, the present study suggests that the combination of LIF/BMP2/FGF2 effectively acts on the maintenance of pluripotency of PSCs as well as on the maintenance of multipotency of NCSCs in the DRGs. LIF/BMP2/FGF2 treatment promoted the proliferation of the DRG cells in both explant and suspension cultures. This treatment also stimulated the proliferation of the DRG cells expressing Oct4. Thus, the combination of these signaling molecules may participate in the proliferation of PSCs in mouse embryonic DRGs.

3. The present data suggest that LIF/BMP2/FGF2 plays important roles not only in the maintenance of multipotency of NCSCs, but also in the maintenance of pluripotency of PSCs in mouse embryonic DRGs. Therefore, we analyzed the relationship between pluripotency-related transcription factors and the factors that characterize mouse NCSCs. The DRG cells expressing both Oct4 and CHD7 were observed *in vivo* and *in vitro*. While the expression of CHD7 and Sox10 was controlled by Oct4, Sox2, and Nanog, the expression of Oct4 was regulated by CHD7. Thus, the expression of pluripotency-related transcription factors in the DRG cells may be regulated by the factors that characterize mouse NCSCs, and vice versa. These findings support the possibility that PSCs in mouse embryonic DRGs are NCSCs and suggest that pluripotency at the early stage of mouse embryonic development is inherited by mouse NCSCs.

## ACKNOWLEDGEMENTS

I would like to thank Dr. Kazuo Ito for his great advices and supports. I would like to thank Dr. Joanna. Wysocka for providing pcDNA3.1 encoding the human WT CHD7 and pcDNA3.1 encoding the human DN CHD7 and to thank Dr. Hidetaka Furuya for advice and help in histochemical staining. I thank Ms. Noriko Takashima and Ms. Yasue Okada for assistance to my student life. Finally, I thank all members of laboratory of Interdisciplinary Biology, my family and my friends for their encouragement. The present works were partly supported by a Sasakawa Scientific Research Grant (26-404) from The Japan Science Society to R. O.

## REFERENCES

Achilleos, A. and Trainor, P. A. (2012). Neural crest stem cells: discovery, properties and potential for therapy. Cell Res. 22, 288-304.

Atari, M., Barajas, M., Hernández-Alfaro, F., Gil, C., Fabregat, M., Ferrés Padró, E., Giner, L. and Casals, N. (2011). Isolation of pluripotent stem cells from human third molar dental pulp. Histol. Histopathol. 26, 1057.

Avilion, A. A., Nicolis, S. K., Pevny, L. H., Perez, L., Vivian, N. and Lovell-Badge, R. (2003). Multipotent cell lineages in early mouse development depend on SOX2 function. Genes Dev. 17, 126-140.

Baggiolini, A., Varum, S., Mateos, J. M., Bettosini, D., John, N., Bonalli, M., Ziegler, U., Dimou, L., Clevers, H., Furrer, R. and Sommer, L. (2015). Premigratory and migratory neural crest cells are multipotent in vivo. Cell Stem Cell 16(3), 314-322.

Bajpai, R., Chen, D. A., Rada-Iglesias, A., Zhang, J., Xiong, Y., Helms, J., Chang, C.-P., Zhao, Y., Swigut, T. and Wysocka, J. (2010). CHD7 cooperates with PBAF to control multipotent neural crest formation. Nature 463, 958-962.

Bengtsson, H., Söderström, S., Kylberg, A., Charette, M. F. and Ebendal, T. (1998). Potentiating interactions between morphogenetic protein and neurotrophic factors in developing neurons. J. Neurosci. Res. 53, 559-568.

Besnard, V., Wert, S. E., Hull, W. M. and Whitsett, J. A. (2004). Immunohistochemical localization of Foxa1 and Foxa2 in mouse embryos and adult tissues. Gene Expr. Patterns 5, 193-208.

Bronner, M. (2015). Confetti clarifies controversy: neural crest stem cells are multipotent. Cell stem cell 16(3), 217-218.

Bixby, S., Kruger, G. M., Mosher, J. T., Joseph, N. M. and Morrison, S. J. (2002). Cell-intrinsic differences between stem cells from different regions of the peripheral nervous system regulate the generation of neural diversity. Neuron 35, 643-656.

Buitrago-Delgado, E., Nordin, K., Rao, A., Geary, L. and LaBonne, C. (2015). Shared regulatory programs suggest retention of blastula-stage potential in neural crest cells. Science 348, 1332-1335.

Chambers, I., Colby, D., Robertson, M., Nichols, J., Lee, S., Tweedie, S. and Smith, A. (2003). Functional expression cloning of Nanog, a pluripotency sustaining factor in embryonic stem cells. Cell 113, 643-655.

Chen, X., Xu, H., Yuan, P., Fang, F., Huss, M., Vega, V. B., Wong, E., Orlov, Y. L., Zhang, W., Jiang, J. et al. (2008). Integration of external signaling pathways with the core transcriptional network in embryonic stem cells. Cell 133, 1106-1117.

Chen, Z., Liu, C., Patel, A. J., Liao, C. P., Wang, Y. and Le, L. Q. (2014). Cells of origin in the embryonic nerve roots for NF1-associated plexiform neurofibroma. Cancer cell 26(5), 695-706.

Chew, J.L., Loh, Y.H., Zhang, W., Chen, X., Tam, W.L., Yeap, L. S., Li, P., Ang, Y. S., Lim, B. and Robson, P. (2005). Reciprocal transcriptional regulation of Pou5f1 and Sox2 via the Oct4/Sox2 complex in embryonic stem cells. Mol Cell Biol. 25, 6031-6046.

Cui, L., Johkura, K., Yue, F., Ogiwara, N., Okouchi, Y., Asanuma, K. and Sasaki, K. (2004). Spatial distribution and initial changes of SSEA-1 and other cell adhesion-related molecules on mouse embryonic stem cells before and during differentiation. J. Histochem. Cytochem. 52, 1447-1457.

Dahl, J.A. and Collas, P. (2008). A rapid micro chromatin immunoprecipitation assay (ChIP). Nat Protoc. 3, 1032-1045.

Desbaillets, I., Ziegler, U., Groscurth, P. and Gassmann, M. (2000). Embryoid bodies: an in vitro model of mouse embryogenesis. Exp. Physiol. 85, 645-651.

De Los Angeles, A., Ferrari, F., Xi, R., Fujiwara, Y., Benvenisty, N., Deng, H., Hochedlinger, K., Jaenisch, R., Lee, S., Leitch, H. G., Lensch, M. W., Lujan, E., Pei. D., Rossane, J., Wernig, M., Park, P.J., Daley G.Q. (2015). Hallmarks of pluripotency. Nature, 525(7570), 469-478.

D'Ippolito, G., Diabira, S., Howard, G. A., Menei, P., Roos, B. A. and Schiller, P. C. (2004). Marrow-isolated adult multilineage inducible (MIAMI) cells, a unique population of postnatal young and old human cells with extensive expansion and differentiation potential. J. Cell Sci. 117, 2971-2981.

Dupin, E. and Sommer, L. (2012). Neural crest progenitors and stem cells: from early development to adulthood. Dev. Biol. 366, 83-95.

Farkas, L. M., Jászai, J., Unsicker, K. and Krieglstein, K. (1999). Characterization of bone morphogenetic protein family members as neurotrophic factors for cultured sensory neurons. Neuroscience 92, 227-235.

Fujita, K., Ogawa, R., Kawawaki, S. and Ito, K. (2014). Roles of chromatin remodelers in maintenance mechanisms of multipotency of mouse trunk neural crest cells in the formation of neural crest-derived stem cells. Mech. Dev. 133, 126-145.

Gammill, L. S., and Bronner-Fraser, M. (2003). Neural crest specification: migrating into genomics. Nat Rev Neurosci. 4, 795-805.

Hagedorn, L., Suter, U. and Sommer, L. (1999). P0 and PMP22 mark a multipotent neural crest-derived cell type that displays community effects in response to TGF-beta family factors. Development 126, 3781-3794.

Hagiwara, K., Obayashi, T., Sakayori, N., Yamanishi, E., Hayashi, R., Osumi, N., Nakazawa, T. and Nishida, K. (2014). Molecular and cellular features of murine craniofacial and trunk neural crest cells as stem cell-like cells. PLoS ONE 9, e84072.

Hall, B. K. (1999). *The Neural Crest in Development and Evolution*. Springer Science & Business Media, New York.

Hall, A. K. (2006). Rodent sensory neuron culture and analysis. Curr. Protoc. Neurosci. Chapter 3, Unit 3. 19.

Hao, J., Li, T. G., Qi, X., Zhao, D.-F. and Zhao, G. Q. (2006). WNT/β-catenin pathway up-regulates Stat3 and converges on LIF to prevent differentiation of mouse embryonic stem cells. Dev. Biol. 290, 81-91.

Hayashi, K. and Saitou, M. (2013). Generation of eggs from mouse embryonic stem cells and induced pluripotent stem cells. Nat. Protoc. 8, 1513-1524.

Hjerling-Leffler, J., Marmigère, F., Heglind, M., Cederberg, A., Koltzenburg, M., Enerbäck, S. and Ernfors, P. (2005). The boundary cap: a source of neural crest stem cells that generate multiple sensory neuron subtypes. Development 132, 2623-2632.

Hjerling-Leffler, J., AlQatari, M., Ernfors, P. and Koltzenburg, M. (2007). Emergence of functional sensory subtypes as defined by transient receptor potential channel expression. J. Neurosci. 27, 2435-2443.

Hübner, K., Fuhrmann, G., Christenson, L. K., Kehler, J., Reinbold, R., De La Fuente, R., Wood, J., Strauss, J. F., Boiani, M. and Schöler, H. R. (2003). Derivation of oocytes from mouse embryonic stem cells. Science 300, 1251-1256.

Ido, A. and Ito, K. (2006). Expression of chondrogenic potential of mouse trunk neural crest cells by FGF2 treatment. Dev. Dyn. 235, 361-367.

Ito, K., Morita, T. and Sieber-Blum, M. (1993). In vitro clonal analysis of mouse neural crest development. Dev. Biol. 157, 517-525.

Itskovitz-Eldor, J., Schuldiner, M., Karsenti, D., Eden, A., Yanuka, O., Amit, M., Soreq, H. and Benvenisty, N. (2000). Differentiation of human embryonic stem cells into embryoid bodies compromising the three embryonic germ layers. Mol. Med. 6, 88.

John, N., Cinelli, P., Wegner, M. and Sommer, L. (2011). Transforming growth factor β-mediated Sox10 suppression controls mesenchymal progenitor generation in neural crest stem cells. Stem Cells 29, 689-699.

Joseph, N. M., Mukouyama, Y. S., Mosher, J. T., Jaegle, M., Crone, S. A., Dormand, E. L., Lee, K. F., Meijer, D., Anderson, D. J. and Morrison, S. J. (2004). Neural crest stem cells undergo multilineage differentiation in developing peripheral nerves to generate endoneurial fibroblasts in addition to Schwann cells. Development 131, 5599-5612.

Jumabay, M., Abdmaulen, R., Ly, A., Cubberly, M. R., Shahmirian, L. J., Heydarkhan-Hagvall, S., Dumesic, D. A., Yao, Y. and Boström, K. I. (2014). Pluripotent stem cells derived from mouse and human white mature adipocytes. Stem Cells Transl Med. 3, 161-171.

Kléber, M., Lee, H.-Y., Wurdak, H., Buchstaller, J., Riccomagno, M. M., Ittner, L. M., Suter, U., Epstein, D. J. and Sommer, L. (2004). Neural crest stem cell maintenance by combinatorial Wnt and BMP signaling. J. Cell Biol. 169, 309-320.

Koike, M., Kurosawa, H. and Amano, Y. (2005). A round-bottom 96-well polystyrene plate coated with 2-methacryloyloxyethyl phosphorylcholine as an effective tool for embryoid body formation. Cytotechnology 47, 3-10.

Kruger, G. M., Mosher, J. T., Bixby, S., Joseph, N., Iwashita, T. and Morrison, S. J. (2002). Neural crest stem cells persist in the adult gut but undergo changes in self-renewal, neuronal subtype potential, and factor responsiveness. Neuron 35, 657-669.

Kukekov, V. G., Laywell, E. D., Thomas, L. B. and Steindler, D. A. (1997). A nestin-negative precursor cell from the adult mouse brain gives rise to neurons and glia. Glia 21, 399-407.

Kurimoto, K., Yabuta, Y., Hayashi, K., Ohta, H., Kiyonari, H., Mitani, T., Moritoki, Y., Kohri, K., Kimura, H., Yamamoto, T. et al. (2015). Quantitative dynamics of chromatin remodeling during germ cell specification from mouse embryonic stem cells. Cell Stem Cell 16, 517-532.

Kurosawa, H. (2007). Methods for inducing embryoid body formation: in vitro differentiation system of embryonic stem cells. J. Biosci. Bioeng. 103, 389-398.

Le Douarin, N. and Kalcheim, C. (1999). *The Neural Crest*. 2nd edn. Cambridge University Press, Cambridge.

Levenstein, M. E., Ludwig, T. E., Xu, R.-H., Llanas, R. A., VanDenHeuvel-Kramer, K., Manning, D. and Thomson, J. A. (2006). Basic fibroblast growth factor support of human embryonic stem cell self-renewal. Stem Cells 24, 568-574.

Li, H.-Y., Say, E. H. M. and Zhou, X. F. (2007). Isolation and characterization of neural crest progenitors from adult dorsal root ganglia. Stem Cells 25, 2053-2065.

Marynka-Kalmani, K., Treves, S., Yafee, M., Rachima, H., Gafni, Y., Cohen, M. A. and Pitaru, S. (2010). The lamina propria of adult human oral mucosa harbors a novel stem cell population. Stem Cells 28, 984-995.

Masui, S., Nakatake, Y., Toyooka, Y., Shimosato, D., Yagi, R., Takahashi, K., Okochi, H., Okuda, A., Matoba, R., Sharov, A. A. et al. (2007). Pluripotency governed by Sox2 via regulation of Oct3/4 expression in mouse embryonic stem cells. Nat. Cell Biol. 9, 625-635.

Mayor, R. and Theveneau, E. (2013). The neural crest. Development. 140(11), 2247-2251.

Mitsui, K., Tokuzawa, Y., Itoh, H., Segawa, K., Murakami, M., Takahashi, K., Maruyama, M., Maeda, M. and Yamanaka, S. (2003). The homeoprotein Nanog is required for maintenance of pluripotency in mouse epiblast and ES cells. Cell 113, 631-642.

Morrison, S. J., White, P. M., Zock, C. and Anderson, D. J. (1999). Prospective identification, isolation by flow cytometry, and in vivo self-renewal of multipotent mammalian neural crest stem cells. Cell 96, 737-749.

Moore, S. W., Sun, K. L. W., Xie, F., Barker, P. A., Conti, M. and Kennedy, T. E. (2008). Soluble adenylyl cyclase is not required for axon guidance to netrin-1. J Neurosci. 28(15), 3920-3924.

Motohashi, T., Kitagawa, D., Watanabe, N., Wakaoka, T. and Kunisada, T. (2014). Neural crest-derived cells sustain their multipotency even after entry into their target tissues. Dev. Dyn. 243, 368-380.

Murphy, M., Reid, K., Hilton, D. J. and Bartlett, P. F. (1991). Generation of sensory neurons is stimulated by leukemia inhibitory factor. Proc. Natl. Acad. Sci. USA. 88, 3498-3501.

Murphy, M., Reid, K., Brown, M. A. and Bartlett, P. F. (1993). Involvement of leukemia inhibitory factor and nerve growth factor in the development of dorsal root ganglion neurons. Development 117, 1173-1182.

Murphy, M., Reid, K., Ford, M., Furness, J. B. and Bartlett, P. F. (1994). FGF2 regulates proliferation of neural crest cells, with subsequent neuronal differentiation regulated by LIF or related factors. Development 120, 3519-3528.

Nagoshi, N., Shibata, S., Kubota, Y., Nakamura, M., Nagai, Y., Satoh, E., Morikawa, S., Okada, Y., Mabuchi, Y., Katoh, H. et al. (2008). Ontogeny and multipotency of neural crest-derived stem cells in mouse bone marrow, dorsal root ganglia, and whisker pad. Cell Stem Cell 2, 392-403.

Nichols, J., Zevnik, B., Anastassiadis, K., Niwa, H., Klewe-Nebenius, D., Chambers, I., Schöler, H. and Smith, A. (1998). Formation of pluripotent stem cells in the mammalian embryo depends on the POU transcription factor Oct4. Cell 95, 379-391.

Niwa, H. (2007). How is pluripotency determined and maintained? Development 134, 635-646.

Niwa, H., Miyazaki, J. I. and Smith, A. G. (2000). Quantitative expression of Oct-3/4 defines differentiation, dedifferentiation or self-renewal of ES cells. Nat. Genet. 24, 372-376.

Niwa, H., Ogawa, K., Shimosato, D. and Adachi, K. (2009). A parallel circuit of LIF signalling pathways maintains pluripotency of mouse ES cells. Nature 460, 118-122.

Nordhoff, V., Hübner, K., Bauer, A., Orlova, I., Malapetsa, A., Schöler, H.R. (2001). Comparative analysis of human, bovine, and murine Oct-4 upstream promoter sequences. Mamm Genome. 12, 309-317.

Ogawa, K., Nishinakamura, R., Iwamatsu, Y., Shimosato, D. and Niwa, H. (2006). Synergistic action of Wnt and LIF in maintaining pluripotency of mouse ES cells. Biochem. Biophys. Res. Commun. 343, 159-166.

Ohinata, Y., Ohta, H., Shigeta, M., Yamanaka, K., Wakayama, T. and Saitou, M. (2009). A signaling principle for the specification of the germ cell lineage in mice. Cell 137, 571-584.

Ota, M. and Ito, K. (2006). BMP and FGF-2 regulate neurogenin-2 expression and the differentiation of sensory neurons and glia. Dev. Dyn. 235, 646-655.

Pan, G. and Thomson, J. A. (2007). Nanog and transcriptional networks in embryonic stem cell pluripotency. Cell Res. 17, 42-49.

Paratore, C., Hagedorn, L., Floris, J., Hari, L., Kleber, M., Suter, U. and Sommer, L. (2002). Cell-intrinsic and cell-extrinsic cues regulating lineage decisions in multipotent neural crest-derived progenitor cells. Int. J. Dev. Biol. 46, 193-200.

Park, K. S., Wells, J. M., Zorn, A. M., Wert, S. E. and Whitsett, J. A. (2006). Sox17 influences the differentiation of respiratory epithelial cells. Dev. Biol. 294, 192-202.

Schnetz, M. P., Handoko, L., Akhtar-Zaidi, B., Bartels, C. F., Pereira, C. F., Fisher, A. G., Adams, D. J., Flicek, P., Crawford, G. E., LaFramboise, T. et al. (2010). CHD7 targets active gene enhancer elements to modulate ES cell-specific gene expression. PLoS Genet. 6, e1001023.

Schroeder, I. S., Sulzbacher, S., Nolden, T., Fuchs, J., Czarnota, J., Meisterfeld, R., Himmelbauer, H. and Wobus, A. M. (2012). Induction and selection of Sox17-expressing endoderm cells generated from murine embryonic stem cells. Cells Tissues Organs 195, 507-523.

Shakhova, O. and Sommer, L. (2010). *Neural crest-derived stem cells.* StemBook. Harvard Stem Cell Institute, Cambridge.

Sieber-Blum, M. (2012). *Neural Crest Stem Cells: Breakthroughs and Applications.* World Scientific, Singapore.

Sieber-Blum, M., Grim, M., Hu, Y. F. and Szeder, V. (2004). Pluripotent neural crest stem cells in the adult hair follicle. Dev. Dyn. 231, 258-269.

Suzuki, N., Yamazaki, S., Yamaguchi, T., Okabe, M., Masaki, H., Takaki, S., Otsu, M. and Nakauchi, H. (2013). Generation of engraftable hematopoietic stem cells from induced pluripotent stem cells by way of teratoma formation. Mol. Ther. 21, 1424-1431.

Takahashi, K. and Yamanaka, S. (2006). Induction of pluripotent stem cells from mouse embryonic and adult fibroblast cultures by defined factors. Cell 126, 663-676.

Tanaka, S. S., Kojima, Y., Yamaguchi, Y. L., Nishinakamura, R. and Tam, P. P. L. (2011). Impact of WNT signaling on tissue lineage differentiation in the early mouse embryo. Dev. Growth Differ. 53, 843-856.

Tanimura, N., Saito, M., Ebisuya, M., Nishida, E. and Ishikawa, F. (2013). Stemness-related factor Sall4 interacts with transcription factors Oct-3/4 and Sox2 and occupies Oct-Sox elements in mouse embryonic stem cells. J Biol Chem. 288, 5027-5038.

Teillet, M. A., Kalcheim, C. and Le Douarin, N. M. (1987). Formation of the dorsal root ganglia in the avian embryo: segmental origin and migratory behavior of neural crest progenitor cells. Dev Biol. 120(2), 329-347.

Thomas, S., Thomas, M., Wincker, P., Babarit, C., Xu, P., Speer, M. C., Munnich, A., Lyonnet, S., Vekemans, M. and Etchevers, H. C. (2008). Human neural crest cells display molecular and phenotypic hallmarks of stem cells. Hum. Mol. Genet. 17, 3411-3425.

Thomson, J. A., Itskovitz-Eldor, J., Shapiro, S. S., Waknitz, M. A., Swiergiel, J. J., Marshall, V. S. and Jones, J. M. (1998). Embryonic stem cell lines derived from human blastocysts. Science 282, 1145-1147.

Tomioka, M., Nishimoto, M., Miyagi, S., Katayanagi, T., Fukui, N., Niwa, H., Muramatsu, M., Okuda, A. (2002). Identification of Sox-2 regulatory region which is under the control of Oct-3/4-Sox-2 complex. Nucleic Acids Res. 30, 3202-3213.

Tomita, Y., Matsumura, K., Wakamatsu, Y., Matsuzaki, Y., Shibuya, I., Kawaguchi, H., Ieda, M., Kanakubo, S., Shimazaki, T., Ogawa, S. et al. (2005). Cardiac neural crest cells contribute to the dormant multipotent stem cell in the mammalian heart. J. Cell Biol. 170, 1135-1146.

Toyooka, Y., Tsunekawa, N., Akasu, R. and Noce, T. (2003). Embryonic stem cells can form germ cells in vitro. Proc. Natl. Acad. Sci. USA. 100, 11457-11462.

Vallier, L., Alexander, M. and Pedersen, R. A. (2005). Activin/Nodal and FGF pathways cooperate to maintain pluripotency of human embryonic stem cells. J. Cell Sci. 118, 4495-4509.

Vojnits, K., Pan, H., Mu, X. and Li, Y. (2015). Characterization of an injury induced population of muscle-derived stem cell-like cells. Sci. Rep. 5, 17355.

Walshe, J. and Mason, I. (2000). Expression of FGFR1, FGFR2 and FGFR3 during early neural development in the chick embryo. Mech. Dev. 90, 103-110.

Wobus, A. M., Holzhausen, H., Jäkel, P. and Schöneich, J. (1984). Characterization of a pluripotent stem cell line derived from a mouse embryo. Exp. Cell Res. 152, 212-219.

Wong, C. E., Paratore, C., Dours-Zimmermann, M. T., Rochat, A., Pietri, T., Suter, U., Zimmermann, D. R., Dufour, S., Thiery, J. P., Meijer, D. et al. (2006). Neural crest–derived cells with stem cell features can be traced back to multiple lineages in the adult skin. J. Cell Biol. 175, 1005-1015.

Yasunaga, M., Tada, S., Torikai-Nishikawa, S., Nakano, Y., Okada, M., Jakt, L. M., Nishikawa, S., Chiba, T., Era, T. and Nishikawa, S. I. (2005). Induction and monitoring of definitive and visceral endoderm differentiation of mouse ES cells. Nat. Biotechnol. 23, 1542-1550.

Ying, Q. L., Nichols, J., Chambers, I. and Smith, A. (2003). BMP induction of Id proteins suppresses differentiation and sustains embryonic stem cell self-renewal in collaboration with STAT3. Cell 115, 281-292.

Yoshida, S., Shimmura, S., Nagoshi, N., Fukuda, K., Matsuzaki, Y., Okano, H. and Tsubota, K. (2006). Isolation of multipotent neural crest-derived stem cells from the adult mouse cornea. Stem Cells 24, 2714-2722.

Zhang, P. L., Levy, A. M., Ben-Simchon, L., Haggiag, S., Chebath, J. and Revel, M. (2007). Induction of neuronal and myelin-related gene expression by IL-6-receptor/IL-6: a study on embryonic dorsal root ganglia cells and isolated Schwann cells. Exp. Neurol. 208, 285-296.

Zorn, A. M. and Wells, J. M. (2009). Vertebrate endoderm development and organ formation. Annu. Rev. Cell Dev. Biol. 25, 221.

# RESEARCH ACHIEVEMENT

## Publications

(1) Ryuhei Ogawa, Kyohei Fujita, Kazuo Ito (2017). Mouse embryonic dorsal root ganglia contain pluripotent stem cells that show features similar to embryonic stem cells and induced pluripotent stem cells. Biology Open, 6, 602-618.

(2) Kyohei Fujita, Ryuhei Ogawa, Kazuo Ito (2016). CHD7, Oct3/4, Sox2, and Nanog control FoxD3 expression during mouse neural crest-derived stem cell formation. The FEBS Journal, 283, 3791-3806.

(3) Kyohei Fujita•, Ryuhei Ogawa•, Syunsaku Kawawaki, Kazuo Ito (2014). Roles of chromatin remodelers in maintenance of multipotency of mouse trunk neural crest cells in the formation mechanisms of neural crest-derived stem cells. Mechanisms of Development. 133, 126-145. (• Both authors contributed equally to this paper.)

**Conference presentation**

(1) 藤田恭平, 小川竜平, 伊藤一男, マウス神経堤細胞由来幹細胞の形成・維持機構, 2P0513, 第 39 回日本分子生物学会年会, 横浜, 2016 年 11 月

(2) 小川竜平, 藤田恭平, 伊藤一男, LIF/BMP2/FGF2 によるマウス後根神経節内神経冠細胞由来多能性幹細胞の分化能維持と増殖, 1P0974, 第 38 回日本分子生物学会年会, 神戸, 2015 年 12 月

(3) 藤田恭平, 小川竜平, 伊藤一男, マウス神経冠細胞由来幹細胞の形成機構, 1P0972, 第 38 回日本分子生物学会年会, 神戸, 2015 年 12 月

(4) Ryuhei Ogawa, Kyohei Fujita, Kazuo Ito (2015). Characterization of neural crest-derived stem cells in mouse dorsal root ganglia. Finnish-Japanese joint symposium on Morphogenesis and Signaling, University of Helsinki, Finland, March 3-4.

(5) 小川竜平, 伊藤一男, マウス神経冠細胞由来幹細胞での CHD7 と Oct4 の共発現, 第 85 回日本動物学会, 仙台, 2014 年 9 月

(6) Kyohei Fujita, Ryuhei Ogawa, Syunsaku Kawawaki, Kazuo Ito (2013). Roles of chromatin remodelers in maintenance of multipotency of mouse trunk neural crest cells in the formation mechanisms of neural crest-derived stem cells. Gordon

Research Conference on Neural Crest & Cranial Placodes, Stonehill collage, Easton, MA, July 21-26.

(7) Kyohei Fujita, Ryuhei Ogawa, Syunsaku Kawawaki, Kazuo Ito, The roles of chromatinremodelers in the maintenance of multipotency of mouse trunk neural crest cells in the relationship with the formation mechanisms of neural crest-derived stem cells, FT4-03, 第 46 回日本発生生物学会年会, 島根, 2013 年 5 月

(8) Kyohei Fujita, Ryuhei Ogawa, Syunsaku Kawawaki, Kazuo Ito, The roles of chromatin remodelers in the maintenance of multipotency of mouse trunk neural crest cells in the relationship with the formation mechanisms of neural crest-derived stem cells, P-049, 第 46 回日本発生生物学会年会, 島根, 2013 年 5 月

(9) 小川竜平, 藤田恭平, 伊藤一男, マウス神経冠細胞の未分化状態維持におけるクロマチンリモデラーCHD7 の役割, 第 83 回日本動物学会, 3L1030, 大阪, 2012 年 9 月